acp-2016-718:

Reply to all comments

The authors would like to thank the reviewers for their thoughtful and helpful comments and suggestions. Their reviews have made a significant contribution to the improvement of the paper. The line numbering in the reviewers' comments refers to the manuscript published in ACPD whereas the line numbering in the responses refers to the new version of the manuscript.

Answer to general comments of both Anonymous Referees:

First of all, as first author, I have to apologize to the referees and the co-authors because I submitted an old version of the manuscript to the ACPD. I submitted the manuscript under pressure and thus I did not realized of my mistake. I would like to clarify that it was completely my fault and nothing related to the co-authors who have widely contribute to this work. I would like to thank the referees for paying attention to the scientific content of the manuscript despite the problems and for giving us the opportunity of replying.

The questions and comments from the Referees (in blue) are answered below (in green).

Answers to Anonymous Referee #1:

General comments:

Secondly, I think the statement made for the improvement of the PBL height is to strong. The methodology sounds very interesting, but is in my opinion limited to situations with Saharan dust intrusions as shown in the 2 case studies of Charmex. Therefore, general statements should be avoided. Instead it should be written that for the meteorological conditions like in Granada this methodology could be a significant improvement. As no long-term data set (>12 months is presented), one can only speculate that the new methodology is a significant improvement. Therefore some statements should be weakened. E.g: the statement in the introduction: P3,l3: "POLARIS improves the zPBL detection since the computation of..." is only valid, IF different aerosol with different depolarization characteristics are existing within and above the PBL. This is certainly not true for many sites not influenced by dust. Or: P5: line 19:"...able to detect the PBL height even when advected aerosol layers in the free troposphere are coupled to the PBL." Only if the advected aerosol layer show a different depolarization ratio.

This methodology can be applied in all stations affected by dust outbreaks which includes, at least, all the Mediterranean countries. This methodology is theoretically valid if different aerosol with different depolarization characteristics are present within and above the PBL. However, in the present study, it has been validated only for dust cases and further analysis with different aerosol types is needed to quantify the improvement. Taking into account this consideration, we have revised the whole document removing the strongest sentences.

-Also the quality of Figures 6 and 7 must be improved. With the current state the discussion is hard to follow. Symbols should be revised for better readability, time scale should have more tick marks, height scale should be probably revised. Often symbols lay very close to each other and have similar color. Reducing symbol frequency could be also an option to consider. Please do definitely choose a different symbol for the PBL top height with POLARIS. The star is not visible and all other symbols are much more prominent.

Figure has been updated following the suggestions of the Anonymous Referees #1 and #2.

-Even so referred to a previous paper I miss a real discussion on the MWR PBL height trust worthiness. In this paper it is always taken as the truth and one wonders why to use the lidar at all...

In this study, the optimization and validation of a new methodology to determine the PBL height has to be performed against a PBL height derived from independent measurements. Thus, we use the PBL height derived from MWR temperature profiles. We have modified the manuscript to highlight that the reference PBL includes also uncertainties and weak points in the methodology.

- An lidar instrument discussion is needed: How trustworthy are profiles close to the lidar (overlap issue but also polarization properties).

The following discussion has been included except the figure: '*The optical path of the parallel and perpendicular channels at 532 nm are designed to be identical up to the PBC where the 532 nm signal is split into parallel and perpendicular before reaching the PMT. This setup allows us to assume almost the same overlap for both polarizing components. Thus, the depolarization profile is practically not influenced by the incomplete overlap since it is cancelled out by the ratio of the perpendicular and parallel channels. Only the thermal dilation and contraction of the lidar optics after the PBC might independently change the overlap function of each channel. Since MULHACEN is deployed inside an air-conditioned building, the temperature fluctuation is small and thus, the overlap difference between the channels might be low. Therefore, we assume significant differences only for small values of the overlap function. Navas-Guzman et al. (2011) and Rogelj et al. (2014) retrieve the overlap function of the total signal at 532 nm (sum of parallel and perpendicular channels) by means of the method presented by Wandinger et al. (2000). This study shows that the full-overlap height of MULHACEN is around 0.72 km agl. Assuming that the artefacts due to thermal fluctuations are negligible for overlap-function values above 70%,*

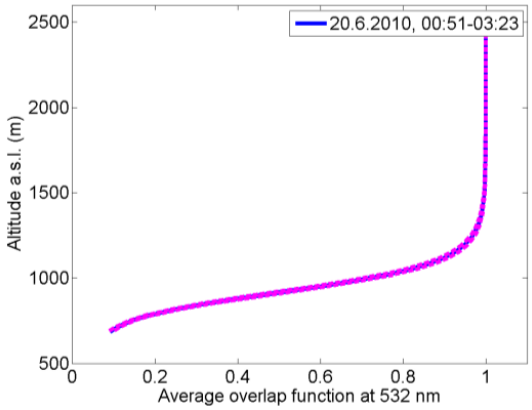

Figure 1: MULHACEN overlap function at 532 nm. Extracted from Rogelj et al., 2014. Station height 680 m asl.

depolarization profiles can be exploited in terms of MLH detection above ~0.25 km agl. Further details about the technical specifications of MULHACEN are provided by Guerrero-Rascado et al. (2008, 2009).'

About the polarization properties, it has been included a reference (Bravo-Aranda, et al., 2016) where the systematic errors of the volume linear depolarization ratio determined with MULHACEN and other lidars in the EARLIENT network are explained in detail. Among others, the most important lidar parameter that can affect the depolarization retrieval is the diattenuation of the receiving optics which is well characterized in MULHACEN. However, these parameters affects to the depolarization calibration which is not required by POLARIS.

Figure: Rogelj et al. 2014: Experimental determination of UV- and VIS- lidar overlap function. Opt. Pura Apl. 47 (3) 169-175.

- Title: I think the title is not representative for the paper as it not only deals with POLARIS. Probably, the model comparison approaches and MWR should be accounted for in the title.

The title has been changed by '*A new methodology for PBL height estimations based on lidar depolarisation measurements (POLARIS): analysis and comparison against microwave radiometer and WRF model based results'*.

-Section 5 should be shortened: Please only show up with new information an restrict to WRF. Almost no new information with respect to the other already published results of R. Banks are given. Probably use WRF to check consistency of retrievals (begin of convection etc.,)

According to the suggestion of the Referee, we have shortened Section 5. Unfortunately, references about PBL height detection using WRF are mainly centered in suitable situations (no clouds, stable, aerosol-free free troposphere) and thus, the comparison with other studies become difficult. The beginning and end of the convection is discussed in the manuscript.

Specific comments (no spelling mistakes):
Page 5, line 11. Unit missing after 0.05 and later in the manuscript. Or what do you mean with dilation parameter?

The unit of the dilation parameter (i.e., kilometer). It has been specified through the manuscript.

Page 5, line 21: What do you mean: can be applied to lidars not fully characterized? I think this is a very "dangerous" statement.

We agree with the referee that the sentence is not appropriate. We meant that the depolarization calibration is not required. The sentence has been changed by: '*Since POLARIS is based on vertical relative changes, the depolarization calibration is not required facilitating the procedure*'.

Page 6: line 12: how can you assure, that this increase is not due to instrumental effects? The ratio of two signals very close to the lidar might not cancel out all instrumental effects anymore, especially regarding depolarization. Do you have a case study where it is seen that the depolarization ratio is constant throughout the atmosphere? I
always see an increase towards ground below 1 km.

The discussion about the overlap effect has been included in a previous comment.

Page 6, line: I did not understand what you mean with lowest layer, please rephrase: "Then, we define two layers: from the full-overlap height up to the lowest candidate, and from the lowest layer up to the highest candidate."

According to the comment, the phrase has been changed by: '*from 120 m agl up to the lowest candidate, and the layer between the lowest and the highest candidate*'.

Page 6, line 26: I do not know what you mean with aerosol stratification in this context, can you explain better?

We assume that the Referee makes reference to the Page 7/line 26. We have changed these phrases for the sake of clarity: '*According to Angelini et al. (2009), occasional aerosol stratification may occur within the mixing layer. This type of stratification which are usually short in time are not really linked with the planetary boundary development leading a false detections of the PBL height. A 7 bin moving median filter is used to reject the possible attributions related to this type of aerosol stratification.*'

Page 7, line 4 to 6. Are these thresholds really without dimension?

They are dimensionless. It has been specified through the manuscript.

Page 8, line 11: An offset of 300 m is not too small, how reliable are the MWR measurements during night time? And how reliable is your lowest candidate, as it is very close to the lidar. I wonder if the depolarization measurements are reliable (see comment above), please discuss this. Especially as you state that Polaris improves the detection. I cannot follow this discussion, as I do not know the "truth".

These differences can be explained considering the different tracers of both methods, and the fact that the POLARIS and MWR are detecting the residual and stable layer top, respectively. The discussion of this paragraph has been changed and a typo in the offset has been corrected: *'The offset of 600 m observed between* z_{SL}^{MWR} *and* z_{RL}^{POL} *during the night is mostly due to the fact that* z_{RL}^{POL} *corresponds to the residual layer and* z_{RL}^{MWR} *marks the top of the nocturnal stable layer.'*

Page 8, line 22. Between 11:20 and 11:30 UTC on which day? Again it is hard to follow, because the symbols are so tiny and especially the Polaris an (star) is almost invisible.

We have rephrased some sentences and included include the date to help the reader to follow the arguments: '*For example, on 16 June 2013, z_{ML}^{MWR} increases from 0.8 km to 2.02 km agl between 10:15 and 11:30 UTC whereas z_{ML}^{POL} increases abruptly from 0.52 to 1.82 km agl between 11:20 and 11:30 UTC (i.e., almost one hour later)*'. Also, the figure has been improved.

Page 8: Discrepancies between MWR and Polaris on 16 June afternoon should be more intensively discussed. I see a systematic bias of almost 1 km.

We agree with the Referee and the discussion has been improved including the difference noted by the Referee among others: '*For example, on 16 June 2013, z_{ML}^{MWR} increases from 0.8 km to 2.02 km agl between 10:15 and 11:30 UTC whereas z_{ML}^{POL} increases abruptly from 0.52 to 1.82 km agl between 11:20 and 11:30 UTC (i.e., almost one hour later). This is because z_{ML}^{MWR} growths due to the increase of the temperature at surface level during the morning whereas z_{ML}^{POL} increases later, once the convection processes are strong enough to dissipate the boundary between the mixing and the residual layer. Another example of the influence of the tracer is the 1-km bias between z_{ML}^{POL} and z_{ML}^{MWR} between 18:00 and 21:00 UTC on 16 June 2013. During the late afternoon and early night, the temperature at surface level quickly decreases and the atmospheric stability suddenly changes from instable to stable. This pattern is registered by the z_{ML}^{MWR} decreasing from 1.82 km to 0.055 km agl between 18:00 and 18:30 UTC. The increasing atmospheric stability during the late afternoon and early night stops the convection processes and then the mixing layer becomes the residual layer. This change from mixing to residual layer is tracked by the temporal evolution of z_{RL}^{POL} decreasing from 1.92 km to 0.52 km agl between 18:00 and 24:00 UTC. Therefore, there are differences between z_{PBL}^{POL} and z_{PBL}^{MWR} explained in terms of the tracer used for each method that are not related to a wrong attribution of POLARIS.*'

Page 9, line 22ff: Does the MWR really watch the same atmospheric column or is scanning included? Then the discussion could be different. Furthermore, also the overlap issue and the near-range depolarization issues could play a role.

HATPRO uses a combination of the scanning mode (measurements at 5.4°, 10.2°, 19.2°, 30°, 42° y 90°) near the surface, below 2 km, and zenithal mode above, since Crewell and Lohnert (2007) showed that these elevation scanning measurements increase the accuracy of the retrieved temperature, specifically in the boundary layer. Thus, we might initially consider that the MWR and the lidar are not exploring the same atmospheric column. However, the channels used during the scanning mode are more opaque (frequencies larger than 54GHz) and thus, the received radiation comes from the nearest layers (i.e., nearest to the zenithal observation). Conversely, the more transparent channels, providing information from the far field, are used during the zenithal observations. Taking into account this information, we do not think that the scanning mode is relevant for the analyses.

Page 11 line 31: These are certainly no long-term measurements, use better continuous measurements

Done.

Page 12, line 7ff: POLARIS allows better model validation compared to what?

We have rephrased the sentence: '*Since POLARIS allows detecting reliable PBL heights under Saharan dust outbreaks, it might be used for the improvement of the WRF parametrization.*'

Fig. 5 please move legend to case B and enlarge - it is not readable even at 150% zoom. Sometimes the blue star changes the color? If the star is overlaid with a dot please make it visible.

Done. Figure 5 has been improved.

Fig. 6 and 7. See above: Poor quality, work on improvement, otherwise discussion cannot be followed. Explanation for WRF missing in caption.

Done. Figure 6 and 7 has been improved.

Fig. 8: pink dot is somewhere else in legend

Done. Figure 8 has been improved.

Answers to Anonymous Referee #2:

The present version of Bravo-Aranda's paper, however, suffers from several short-comings. First, the small set of measurements is problematic. As a consequence, it cannot be demonstrated in a convincing way that POLARIS is useful when long time series shall be evaluated. Even for the short period of only 3 days (according to doi:10.5194/acp-16-455-2016, the SOP I of ChArMEx 2013 took place from 11. June to 5. July: what about this data-set?) a lot of situations were found when the different methodologies disagree. It is also not clear whether the basic assumption (if I understand it correctly, unfortunately it is not sufficiently explained) "a depolarizing aerosol layer is a transported desert dust layer and does not belong to the mixing layer" can be applied to other sites than Granada (or other Mediterranean countries). So this paper (provided the text has been undergone a substantial revision in grammar and spelling, and has been improved in terms of scientific clarity) can only be considered as a first contribution to a discussion of the benefit of adding depolarization-information to a MLH-retrieval.

Despite the ChArMEx campaigns took place from 11 June to 5 July 2013, the continuous lidar measurements were scheduled from 9 to 11 July 2012 (~72 hours) and from 16 to 17 June 2013 (~36 hours). We use these continuous lidar measurements under Saharan dust outbreaks to analyze the temporal evolution of the PBL. Also, the periods are large enough to demonstrate how POLARIS improves the detection with respect to the method which uses only the RCS and to evidence that the depolarization measurements is useful for the detection of the PBL height.

Despite POLARIS is validated using dust layers coupled to the PBL, a priori, it can be used for any layer coupled to the PBL if the aerosol particle-shape is different enough to be detected by the depolarization profile. For example, a dust layer coupled to the PBL which is a frequent scenario in all the Mediterranean countries as well as in those regions affected by dust outbreaks. POLARIS represents a real improvement compared to previous methodologies used for the automatic detection of the PBL height based on lidar data using only the RCS, which tended to erroneously estimate the PBL top under complex situations. As observed in the manuscript, much lower differences are observed between z_{PBL}^{POL} and the reference (z_{PBL}^{MWR}) than between C_{RCS} and z_{PBL}^{MWR}. Nonetheless, discrepancies still exist between the PBL height determined with the MWR and POLARIS, but they can be easily explained taking into account the use of different tracers (i.e. temperature and aerosol) and the uncertainties associated to both methodologies. The text in the manuscript has been modified accordingly.

I will not list the countless typos, word repetitions, cases of wrong grammar, misuse of capital letters, misspelled units, or undefined symbols. Even one of the affiliations is not correct and the link to the ChArMEx-Website does not work! Only a few specific mostly sci ence-related issues are listed below. In summary I think the authors should take all comments seriously. If not all issues are fully resolved I will not recommend the publication of a revised version.

Specific comments:

• page 2, lines 14ff: There is an extensive discussion on different regimes as the residual layer, the mixing layer, the convective boundary layer and more. In the rest of the paper primarily the "PBL" is mentioned and discussed (see 3/5). A strict terminology is required throughout the paper. When there is a co-existence of the residual layer and the convective layer (e.g. after sunrise) PBL might be confusing.

The advice of the Referee has been taking into account and thus, the discussion of the results has been updated according to the PBL type (e.g., mixing layer, residual layer and stable layer) through the manuscript.

• 2/23: "Sunrise and Sunset are characterized by the complexity of the PBL.": This sentence is really strange!

We agree with the referee that the sentence is not appropriated. The sentence has been changed by: *'The PBL structure is especially complex during the sunrise and sunset when the mixing and residual layers may coexist'*.

• 3/18: "... are feasible and reliable ...": What is meant with "reliable"? In the paper many example are shown when this is not the case.

The word ‘reliable’ has been removed and the text has been rewritten: ‘*Since the experimental detection of z_{PBL} is spatially and temporally limited due to instrumental coverage, the use of Numerical Weather Prediction (NWP) models for the estimation of z_{PBL} is a feasible alternative*’.

• 3/21: "... include stringent conditions ...": What is this?

The text has been modified and thus, the word ‘stringent’ has been removed: ‘*Since the experimental detection of z_{PBL} is spatially and temporally limited due to instrumental coverage, the use of Numerical Weather Prediction (NWP) models for the estimation of z_{PBL} is a feasible alternative. In this regard, several validation studies of these model estimations have been conducted based on lidar and surface and upper air measurements (Dandou et al., 2009; Helmis et al, 2012), some of them in areas close to the study region (Borge et al., 2008; Banks et al., 2015). Results showed that NWP estimations of the z_{PBL} (z_{PBL}^{WRF}) are feasible, but with a tendency to the underestimation of the z_{PBL} in most synoptic conditions. In this study, z_{PBL}^{WRF} is tested against the z_{PBL} derived from POLARIS and MWR measurements under Saharan dust events*’.

• 4/8: There are a lot of words on the overlap, but the most relevant number, i.e. the minimum range that can be exploited in terms of MLH, is missing. Why is the 90% overlap-range given as a interval? Is it temperature dependent? If it depends on the channel (i.e., wavelength) but only one wavelength is used in this study, it is not adequate to give a range. It is strange that the polarization channels which are the most relevant in view of the novelty of POLARIS are not mentioned here – whereas the irrelevant Raman- channels and water vapor channels are mentioned.

We agree with the Referee. We have included more information about the overlap of the polarizing channels and discussed the possible influences on the measurements as follows: ‘*The optical path of the parallel and perpendicular channels at 532 nm are designed to be identical up to the PBC where the 532 nm signal is split into parallel and perpendicular before reaching the PMT. This setup allows us to assume almost the same overlap for both polarizing components. Thus, the depolarization profile is practically not influenced by the incomplete overlap since it is cancelled out by the ratio of the perpendicular and parallel channels. Only the thermal dilation and contraction of the lidar optics after the PBC might independently change the overlap function of each channel. Since MULHACEN is deployed inside an air-conditioned building, the temperature fluctuation is small and thus, the overlap difference between the channels might be low. Therefore, we assume significant differences only for small values of the overlap function. Rogelj et al. (2014) retrieve the overlap function of the total signal at 532 nm (sum of parallel and perpendicular channels) by means of the method presented by Wandinger et al. (2000). This study shows that the full-overlap height of MULHACEN is around 0.72 km agl. Assuming that the artefacts due to thermal fluctuations are negligible for overlap-function values above 70%, depolarization profiles can be exploited in terms of MLH detection above ~0.25 km agl. Further*

details about the technical specifications of MULHACEN are provided by Guerrero-Rascado et al. (2008, 2009).'

• 4/28: The vertical resolution given here does not agree with the statement in line 21.

We have removed the vertical resolution on that sentence and rephrased that paragraph as follows: '*The MWR temperature profile is used to locate the* z_{PBL} (z_{PBL}^{MWR}) *by two algorithms. Under convective conditions, fuelled by solar irradiance absorption at the surface and the associated heating, the parcel method is used to determine the mixing layer height* z_{ML}^{MWR} *(Holzworth, 1964). Granados-Muñoz et al. (2012) already validated this methodology obtaining good agreement with radiosonde measurements. Since the parcel method is strongly sensitive to the surface temperature (Collaud-Coen et al., 2014), surface temperature data provided by the MWR are replaced by more accurate temperature data from a collocated meteorological station, in order to minimize the uncertainties in* z_{ML}^{MWR} *estimation. Conversely, under stable situations, the stable layer height* z_{SL}^{MWR} *is obtained from the first point where the gradient of potential temperature (*ϑ*) equals zero. Collaud-Coen et al. (2014) determine the uncertainties of the PBL height for both methods by varying the surface temperature by ±0.5°. The uncertainties are on the order of ±50 to ±150 m for the PBL maximum height reached in the early afternoon, although uncertainties up to ±500 m can be found just before sunset. Further details about both methods are given by Collaud-Coen et al. (2014).'*

• 5/24: "both ... are normalized respectively to the maximum value of RCS and δ in the first kilometer above the surface ". In case of δ no normalization can be seen in any of the corresponding figures. Please clarify.

The correct normalized δ profile has been included in all the axes of Figure 5.

• section 3: It is not common to use the character "C" for a height.

We agree that the character is not commonly used as height but we need to distinguish between the candidates and the final PBL height. Thus, we decide to use 'C' for the candidates where the subscript makes reference to the type of candidate as listed in the point 2) of the Section 3.2:

i. C_{RCS}*: the height of the* W_{RCS} *maximum closest to the surface exceeding a certain threshold* η_{RCS}*. This threshold is iteratively decreased, starting in 0.05, until* C_{RCS} *is found. This is procedure established by Granados-Muñoz et al. (2012). A dilation value (*a_{RCS}*) of 0.03 km is used according to Granados-Muñoz et al. (2012).*
ii. C_{min}*: the height of the* W_{δ} *minimum closest to the surface exceeding the threshold* η_{min}*.* C_{min} *indicates the height of the strongest increase of δ.*
iii. C_{max}*: the height of the* W_{δ} *maximum closest to the surface exceeding the threshold* η_{max}*.* C_{max} *indicates the height of the strongest decrease of δ.*

and ‘z’ is used for the final PBL where the superscript makes reference to the method (i.e., ‘POL’, ‘MWR’, ‘WRF’). We think that the sentences in Section 2 adequately highlights that the symbol ‘C’ makes reference to the height of the candidates.

• 6/4: Fig. 6 is discussed prior to Figs. 4 and 5. Fig. 3 is missing!

We have changed the numeration of the figures.
Page 4/L19: Fig. 1
Page 4/L20: Fig. 2
Page 5/L12: Fig. 3
Page 5/L15: Fig. 4
Page 6/L18: Fig. 5
Page 6/L26: Fig. 6
Page 7/36: Fig. 7

• 6/5: What is the reason for selecting RCS at 532 nm? Furthermore, "height above mean sea level" should be transformed to "height above ground" (throughout the paper).

We decided to plot the RCS and the δ at the unique wavelength with depolarization capability (532 nm).

• 6/8: "We do not expect the ...": Does this mean that an automated POLARIS retrieval is not possible?

The sentence is confusing and thus, it was removed. Additionally, we have move the point 3) from the methodology to the end of the Section 3.2 where we illustrate how the distribution in height of the candidates is related to a specific atmospheric situation as follows: ‘*To illustrate how the distribution in height of the candidates is related to a specific atmospheric situation, we analyse a particular case at 21:30 UTC on 16 June 2013 (Fig. 5) corresponding to an example of the c.1 scenario. As can be seen, C_{RCS} and C_{max} are located at 4.46 and 4.41 km agl whereas C_{min} is located at 0.7 km agl. Since the different between C_{RCS} and C_{max} is lower than 0.15 km, we assume that both candidates points to the same edge of the layer and thus, this situation corresponds to $C_{RCS} = C_{max} > C_{min}$. The mean and variance of δ in the layer below C_{min} ands the layer between C_{min} and C_{max} are 0.65 and 7·10-4 and 0.99 and 91·10-4, respectively. Since the δ mean difference is larger than δ_t and the variances differ more than 30%, we determine that there are two different layers: the PBL (low δ) and the coupled layer (high δ) where $C_{RCS} = C_{max}$ indicates the coupled layer top and C_{min} indicates the limit between the residual and the coupled layer, being chosen as z_{PBL}. In this particular case, POLARIS improves the z_{PBL} detection from 4.46 agl to 0.7 km agl*’.

• 6/15ff: The following discussion is confusing. A few examples: Under "b.1" it is stated that CRCS =Cmax (by the way another typo: should be C RCS) whereas in the next line of text the authors describe that C CRS =Cmax! It is not clear, what the "lowest layer" is (line 22). It is doubtful that

at the top of a lofted layer RCS increases (7/2), the opposite should be the case. It is not clear why there is an increase of δ "before C max" (7/7). It should be clearly outlined what should be understood by "coupled", it seems that it is used in different ways.

The whole Section 3.2 has been rewritten according to the comments of the Referee #2.

It is difficult to understand a situation when C min > Cmax, whereas the opposite can be identified as e.g. a lofted dust layer.

C_{min} > C_{max} means that δ profile has an abrupt decrease (C_{min}) and then, an abrupt increase (C_{max}). This pattern fits with the presence of a lofted layer above the PBL (as considered in the scenario c.2.2). For example, at 06:00 UTC on 11/07/2012 (Fig. 7).

• In Fig. 5 the differences of the profiles in cases D/E or F/G are hardly visible. Nevertheless the retrieval results in quite different zPBL. This seems to be a weakness of the method and should be discussed in detail. Moreover, case I
seems to be critical. The "inhomogeneities" in the shape of the δ-profiles are not much pronounced so it seems questionable if depolarization should be exploited at all, especially when considering measurement errors (error bars are missing in all figures!). The labels of the axes and the legend are hardly readable.

Figures have been improved to facilitate the analysis. The inhomogeneities in the shape of the δ-profiles are strong enough to allow the detection of at least one of the candidates C_{min} and C_{max}. In any case, the absence of both candidates should not be considered as a weakness of the method but a possible scenario in which the depolarization changes are not stronger enough to find an edge and thus, C_{RCS} is chosen as z_{PBL}. The methodology has been changed to include this possibility. However, this change does not affect to the results presented in the manuscript because this situation did not occur. The error bars have been omitted since we do not performed a direct comparison between the profiles. In fact, these figures just illustrate the different candidate height distributions of each scenario.

• Section 3.3: A discussion of how the different thresholds are found is missing. There are only statements on specific numbers. The rest of the text does not really fit to the title of the section; it is rather a discussion of the differences of the old and new method.

More comments about the optimization process has been included to fit the discussion to title of the section.

• 8/16: "CRCS indicates layeringpoints to a weak edge within the PBL. " Another example of a "weird" sentence.

The Section 3.2 has been rewritten according to the comments of the Referee #2.

• 8/21: Why do the authors switch to "m" instead of "km" as in the rest of the text?

We have decided to switch from m to km in the whole manuscript.

• Section 4: Validation is performed by means of the MWR-retrieval. This implies that the latter is assumed to be the truth (see analysis in doi:10.5194/amt-7-3685-2014). As a consequence the MWR-retrieval and its accuracy has to be explained in more detail.

In this study, the optimization and validation of a new methodology to determine the PBL height has to be performed against a PBL height derived from independent measurements. Thus, we use the PBL height derived from MWR temperature profiles. We have modified the manuscript to highlight that the reference PBL includes also uncertainties and weak points in the methodology. Additionally, more information about its accuracy has been included.

In Section 4 the authors demonstrate that there are a lot of differences. Thus, the reader might conclude that the POLARIS-retrieval does not work reliably (in my view the grey and black stars never coincide in Fig. 7). In Fig. 7 it is not explicitly explained which parameter is shown in the upper/lowerpanel.

Figure 7 has been corrected.

• 9/24: There are no red triangles in Fig. 9!

Done. Figure 8 has been improved.

• Section 5: Obviously there are very few cases when POLARIS-retrievals agree with the WRF-simulations. What is the conclusion with respect to the usefulness of POLARIS or the accuracy of WRF?

As reported in the manuscript there has been previous studies evaluating the performance of the WRF model estimating the PBL height. Nevertheless, few of them, if any, have evaluated this performance under the complex conditions here analyzed. As commented in the manuscript, the main differences are found during daytime under the Saharan dust outbreaks, were the WRF model clearly underestimates the PBL height. Although other reason can explain this underestimation (as for instance insufficient number of model layers), the more plausible one is the inability of the here used WRF PBL parameterization to account properly for this particular kind of events. This is the main conclusion regarding the POLARIS and the WRF model. Thus, in future work, other PBL parameterizations may be evaluated. In addition, the here used dataset and the POLARIS method may be used to improve the WRF PBL parameterizations.

A new methodology for PBL height estimations based on lidar depolarisation measurements: analysis and comparison against MWR and WRF model based results

Juan Antonio Bravo-Aranda[1,2,a], Gregori de Arruda Moreira[3], Francisco Navas-Guzmán[4], María José Granados-Muñoz[1,2,b], Juan Luis Guerrero-Rascado[1,2], David Pozo-Vázquez[5], Clara Arbizu-Barrena[6], Francisco José Olmo Reyes[1,2], Marc Mallet[7,c] and Lucas Alados Arboledas[1,2]

[1]Andalusian Institute for Earth System Research (IISTA-CEAMA), Granada, Spain
[2]Dpt. Applied Physics, University of Granada, Granada, Spain
[3]Institute of Energetic and Nuclear Research (IPEN), São Paulo, Brazil
[4]Institute of Applied Physics (IAP), University of Bern, Bern, Switzerland
[5]Dpt. of Physics, University of Jaén, Jaén, Spain
[6]Laboratoire d'Aérologie, Toulouse, France
[7]Centre National de Recherches Météorologiques, Toulouse, France
[a]now at: Institute Pierre-Simon Laplace, CNRS-Ecole Polytechnique, Paris, France
[b]currently at: Table Mountain Facility, NASA/Jet Propulsion Laboratory, California Institute of Technology, Wrightwood, California, USA
[c]now at: CNRM, Météo-France-CNRS, Toulouse, France

Correspondence to: Juan A. Bravo-Aranda (jabravo@ugr.es)

Abstract.

The automatic and non-supervised detection of the planetary boundary layer height (z_{PBL}) by means of lidar measurements was widely investigated during the last years. Despite ~~the~~ considerable advances ~~achieved~~ , the experimental detection still presents difficulties such as ~~either because the PBL is stratified (typically, during night-time) either because~~ advected aerosol layers ~~are~~ coupled to the PBL~~. The coupling~~ which ~~uses~~ usually ~~to~~ produce an overestimation of the z_{PBL}. To improve the detection of the z_{PBL} ~~even~~ in these complex atmospheric situations, we present a new algorithm, called POLARIS (PBL height estimatiOn based on Lidar depolARISation). POLARIS applies the wavelet covariance transform (WCT) to the range corrected signal (RCS) and to the perpendicular-to-parallel signal ratio (δ) profiles. Different candidates for z_{PBL} are chosen and the selection is done, based on the WCT applied to the RCS and the δ. We use two ChArMEx campaigns with lidar and microwave radiometer (MWR) measurements, conducted on 2012 and 2013, for the POLARIS' adjustment and validation. POLARIS improves the z_{PBL} detection compared to previous methods based on lidar measurements, especially when an aerosol layer is coupled to PBL. ~~thanks to the consideration of the relative changes in the depolarization capabilities of the aerosol particles in the lower part of the atmospheric column. Taking the advantage of a proper determination of the z_{PBL} determined by POLARIS and by MWR under Saharan dust events,~~W ~~w~~e also compare the z_{PBL} provided by the Weather Research and Forecasting (WRF) numerical weather prediction model with respect to the z_{PBL} determined with ~~the~~ POLARIS and the MWR ~~z_{PBL} with the z_{PBL} provided by the Weather Research and Forecasting (WRF) numerical weather prediction model~~under Saharan dust events. WRF underestimates the z_{PBL} during daytime but agrees with the MWR during night-time. The z_{PBL} provided by WRF shows a better temporal evolution compared with the MWR during daytime than ~~during night-time~~at night.

1 Introduction

The planetary boundary layer (PBL) is the region of the troposphere directly influenced by the processes at the Earth's surface. This region typically responds to surface forcing mechanisms with a time scale of about one hour or less (Stull, 1988). The PBL height z_{PBL} is a relevant meteorological variable with a strong effect on air pollution as it defines the atmospheric volume

that can be used for pollutant dispersion. Along the time, different approaches based on the use of elastic lidar data have been proposed for detecting the z_{PBL} (e.g., Morille et al., 2007; Granados-Muñoz et al., 2012; Wang et al., 2012; Pal et al., 2013; Coen et al., 2014; Banks et al., 2015). Among them, some methods like the wavelet covariance transform (WCT) have already demonstrated to be a good tool for an automatic and unsupervised detection of the z_{PBL} (Morille et al., 2007; Baars et al., 2008; Pal et al., 2010;Granados-Muñoz et al., 2012; Wang et al., 2012). This method can be considered the combination of applying the so-called gradient method to a range corrected profile after smoothing by a low-pass filter (Comerón et al., 2013). In these methods, the top of the PBL is associated to the height where there is a sharp decrease of the range corrected signal (RCS) and thus of the aerosol load. Lidars provide an interesting tool for the retrieval of the PBL height, due to their vertical and temporal resolution that allows a continuous monitoring of the PBL. In addition, the number of active ceilometers in Europe has considerably increased due to the low cost and the easy maintenance, allowing us to improve the spatial and temporal monitoring of the PBL. Both lidars and ceilometers use aerosol as a tracer for the identification of the PBL height. This represents a challenge due to the PBL evolution and complex internal structure. The diurnal period is characterized by a mixing layer (statically unstable) where ~~Turbulent~~ turbulent mixing controls the vertical dispersion up to the top of the ~~CBL~~ convective cells (Seibert, 2000). The ~~CBL~~ mixing boundary layer ~~is denominated~~ becomes mixed layer, when the homogenization is complete (neutral stability), something that happens when turbulence is really vigorous and there is an intense convection. During night-time, the stable boundary layer (also known as nocturnal boundary layer) is in direct contact with the surface, and the residual layer is located above the stable layer, loaded with the aerosol that reached high elevation in the previous day (Stull, 1988). The PBL structure is especially complex during the ~~Sunrise~~ sunrise and ~~Sunset~~ sunset when the mixing and residual layers coexist~~are characterized by the complexity of the PBL~~. Furthermore, the coupling of advected aerosol layers in the Free Troposphere with aerosol in the PBL or the presence of clouds lead to under- or overestimation of the PBL height (Granados-Muñoz et al., 2012; Summa et al., 2013).

In this work, we present a new method, called POLARIS (PBL height estimatiOn based on Lidar depolARISation), which is an ameliorated version of the method presented by Baars et al., (2008) and Granados-Muñoz et al., (2012). POLARIS uses the combination of the WCT applied to the RCS and the perpendicular-to-parallel signal ratio (δ) profiles. Using these profiles, different candidates for the z_{PBL} are chosen and the optimum candidate is selected using POLARIS algorithm. POLARIS is particularly useful when advected aerosol layers in the free troposphere are coupled to the PBL because the lidar depolarization ratio profiles provide information about the particle shape allowing the discrimination among different aerosol types. Furthermore, POLARIS improves the z_{PBL} detection since the computation of δ (based on the ratio of two lidar signals) partially cancels out the incomplete overlap effect, allowing the z_{PBL} detection at lower heights than using methods based exclusively on the RCS (affected by incomplete overlap). ~~To simplify the nomenclature, hereafter, we will refer to the z_{PBL} understanding the top of the mixing, mixed or residual layer except when needed.~~

Data sets of lidar and ~~Micro Wave~~microwave ~~Radiometer~~ radiometer measurements registered in ChArMEx (Chemistry-Aerosol Mediterranean Experiment, http://charmex.lsce.ipsl.fr/~~www.charmex.lsce.ipsl.fr~~) experimental campaigns during the summers of 2012 and 2013 are used in this study for the POLARIS evaluation. ChArMEx is a collaborative research program federating international activities to investigate Mediterranean regional chemistry-climate interactions (Mallet et al., 2016). One of the goals of ChArMEx is to reach a better knowledge on the atmospheric aerosol over the Mediterranean Basin (Dulac et al., 2014; Sicard et al., 2016; Granados-Muñoz et al., 2016). This work contributes to the Mediterranean studies since POLARIS improves the PBL detection under the frequent dust outbreaks affecting this region.

Since the experimental detection of z_{PBL} is spatially and temporally limited due to instrumental coverage, the use of Numerical Weather Prediction (NWP) models for the estimation of z_{PBL} is a feasible alternative. In this regard, several validation studies of these model estimations have been conducted based on lidar and surface and upper air measurements (Dandou et al., 2009; Helmis et al, 2012), some of them in areas close to the study region (Borge et al., 2008; Banks et al., 2015). Results showed that NWP estimations of the z_{PBL} (z_{PBL}^{WRF}) are feasible ~~and reliable~~, but with a tendency to the underestimation of the z_{PBL} in

most synoptic conditions. In this study, z_{PBL}^{WRF} ~~In this work the WRF (Weather Research and Forecasting) NWP model (Skamarock et al., 2008), z_{PBL} estimations are~~ is tested ~~based~~ against ~~on~~ the z_{PBL} derived from POLARIS ~~algorithm~~and MWR measurements under Saharan dust events. ~~Some of the period here tested include stringent complex conditions, as the presence of an advected aerosol layer coupled to the PBL.~~

2 Experimental site and instrumentation

In this work we use measurements registered in the Andalusian Institute for Earth System Research (IISTA-CEAMA). This center is located at Granada, in Southeastern Spain (Granada, 37.16°N, 3.61°W, 680 m asl). The metropolitan Granada's population is around 350 000 inhabitants: 240 000 inhabitants from the city and 110 000 inhabitants from the main villages surround the city (~~www.ine.es~~www.ine.es). It is a non-industrialized city surrounded by mountains (altitudes up to 3479 m asl, Mulhacén peak). Granada's meteorological conditions are characterized by a large seasonal temperature range (cool winters and hot summers) and by a rainy period between late autumn and early spring with scarce rain the rest of the year.

The main local sources of aerosol particles are the road traffic, the soil re-suspension (during warm-dry season) and the domestic heating based on fuel oil combustion (during winter) (Titos et al., 2012). Additionally, due to its proximity to the African continent, Granada's region is frequently affected by outbreaks of Saharan air masses becoming an exceptional place to characterize Saharan dust. Additionally, Lyamani et al. (2010) and Valenzuela et al. (2012) point to the Mediterranean basin as an additional source of aerosol particles in the region.

MULHACEN is a multiwavelength lidar system with a pulsed Nd:YAG laser, frequency doubled and tripled by Potassium Dideuterium Phosphate crystals. MULHACEN emits at 355, 532 and 1064 nm (output energies per pulse of 60, 65 and 110 mJ, respectively) and registers elastic channels at 355, 532 and 1064 nm and Raman-shifted channels at 387 (from N2), 408 (from H2O) and 607 (from N2) nm. The depolarization measurements are performed by splitting the 532 nm signal by means of a polarizing beam-splitter cube (PBC), being the parallel signal with respect to the polarizing plane of the outgoing laser beam measured in the reflected part of the PBC. The depolarization calibration is performed by means of the ±45◦ calibration method (Freudenthaler et al., 2009). This calibration procedure performed with MULHACEN is described in detail by Bravo-Aranda, et al. (2010) and its systematic errors analysed by Bravo-Aranda, et al. (2016).

~~The laser beam also passes through two beam expanders reducing the divergence and increasing the surface of the laser beam by a factor ×5 and ×4.5 for 355 nm and 532/1064 nm, respectively.~~ The optical path of the parallel and perpendicular channels at 532 nm are designed to be identical up to the PBC where the 532 nm signal is split into parallel and perpendicular before reaching the PMT. This setup allows us to assume almost the same overlap for both polarizing components. Thus, the depolarization profile is practically not influenced by the incomplete overlap since it is cancelled out by the ratio of the perpendicular and parallel channels. Only the thermal dilation and contraction of the lidar optics after the PBC might independently change the overlap function of each channel. Since MULHACEN is deployed inside an air-conditioned building, the temperature fluctuation is small and thus, the overlap difference between the channels might be low. Therefore, we assume significant differences only for small values of the overlap function. Navas-Guzman et al. (2011) and Rogelj et al. (2014) retrieve the overlap function of the total signal at 532 nm (sum of parallel and perpendicular channels) by means of the method presented by Wandinger et al. (2000). This study shows that the full-overlap height of MULHACEN is around 0.72 km agl~~is reached around 1220 m agl for all the wavelengths~~. Assuming that the artefacts due to thermal fluctuations are negligible for overlap-function values above 70%, depolarization profiles can be exploited in terms of MLH detection above ~0.25 km agl. Further details about the technical specifications of MULHACEN are provided by Guerrero-Rascado et al. (2008, 2009).

A ground-based passive microwave radiometer (RPG-HATPRO, Radiometer Physics GmbH) continuously measured tropospheric temperature and humidity profiles during the studied period. The microwave radiometer (MWR) uses direct detection receivers within two bands: 22-31 GHz (providing information about the tropospheric water vapour profile) and 51-

Mis en forme : Anglais (Royaume-Uni)

58 GHz (related to the temperature profile). Temperature profiles are retrieved from surface meteorological and the brightness temperature measured at the V-band frequencies with a radiometric resolution between 0.3 and 0.4 K root mean square error at 1-s integration time. The frequencies 51.26, 52.28 and 53.86 GHz are used only in zenith pointing and the frequencies 54.94, 56.66, 57.3 and 58 GHz are considered for all the elevation angles (Meunier et al., 2013). The inversion algorithm is based on neural networks (Rose et al., 2005) trained using the radiosonde database of the Murcia WMO station nr. 08430 located at 250 km from Granada. The accuracy of the temperature profiles is 0.8 K within the first 2 km and 1.5 K between 2 and 4 km. ~~Vertical resolution~~ The altitude grid of the inversion increases with height: 30 m below 300 m agl, 50 m between 300-1200 m agl, 200 m between 1200 and 5000 m agl and 400 m above ~~.~~ (Navas-Guzmán, 2014). The MWR temperature profile is used to locate the z_{PBL} $\left(z_{PBL}^{MWR}\right)$ by two algorithms. Under convective conditions, fuelled by solar irradiance absorption at the surface and the associated heating, the parcel method is used to determine the mixing layer height z_{ML}^{MWR} (Holzworth, 1964). Granados-Muñoz et al. (2012) already validated this methodology obtaining a good agreement with radiosonde measurements. Since the parcel method is strongly sensitive to the surface temperature (Collaud-Coen et al., 2014), surface temperature data provided by the MWR are replaced by more accurate temperature data from a collocated meteorological station, in order to minimize the uncertainties in z_{ML}^{MWR} estimation. Conversely, under stable situations, the stable layer height z_{SL}^{MWR} is obtained from the first point where the gradient of potential temperature (θ) equals zero. Collaud-Coen et al. (2014) determine the uncertainties of the PBL height for both methods by varying the surface temperature by ±0.5°. The uncertainties are on the order of ±50 to ±150 m for the PBL maximum height reached in the early afternoon, although uncertainties up to ±500 m can be found just before sunset. Further details about both methods are given by Collaud-Coen et al. (2014).

~~). Conversely, under stable situations, $\mathbf{z_{PBL}^{MWR}}$ is obtained from the first point where the gradient of potential temperature (θ) is equal zero. Collaud-Coen et al. (2014) give further details about both methods. Granados-Muñoz et al., 2012 already validated this methodology with radiosonde measurementsobtaining good comparisons with radiosonde measurements. . However, t(Conversely, under stable situations, $\mathbf{z_{PBL}^{MWR}}$ is obtained from the first point where the gradient of potential temperature (θ) is equal zero. Collaud-Coen et al. (2014) give further details about both methods. The he uncertainty of the $\mathbf{z_{PBL}^{MWR}}$ is estimated to be 200 m below 2 km, and 400 m above 2 km. The large uncertainties are because due to of the low vertical resolution of the MWR temperature profile is between 100 and 500 m for heights below 3 km agl, where the PBL is usually located over Granada (Granados-Muñoz et al., 2012). Additionally, the parcel method is strongly sensitive to the surface temperature where a variation of ±1ºC can significantly change the retrieved PBL height. To improve the $\mathbf{z_{PBL}^{MWR}}$ retrieval, we use the surface temperature from a meteorological station instead of the nearest temperature to the surface of the MWR. The error sources of the PBL height determined with the first point where the gradient of potential temperature (θ) is equal zero are X, Y and Z.~~

3 The POLARIS method

3.1Wavelet Covariance Transform

The wavelet covariance transform $W_F(a,b)$ applied to a generic function of height, $F(z)$, (e.g., RCS or δ) is defined as follows:

$$W_F(a,b) = \frac{1}{a}\int_{z_b}^{z_t} F(z)\,h\left(\frac{(z-b)}{a}\right)dz \qquad \text{Eq. 1}$$

where z is the height, z_b and z_t are the integral limits and $h((z-b)/a)$ is the Haar's function defined by the dilation, a, and the translation, b (Fig. 1).

Fig. 2 shows an example of the WCT applied to the RCS (W_{RCS}). W_{RCS} presents a maximum in coincidence with the sharpest decrease of the RCS and thus, the W_{RCS} maximum is associated to a sharp decrease of the aerosol load which could be related

to the top of the PBL. In this sense, Baars et al. (2008) proposed the use of the first maximum in the W_{RCS} profile from surface larger than a threshold value to detect the z_{PBL}. Granados-Muñoz et al. (2012) improved this method using an iterative procedure over the dilation parameter starting at 0.05 km and decreasing with steps of 0.005 km. These studies show that the automatic application of this method provides reliable results of the PBL height in most cases. However, Granados-Muñoz et al. (2012) state that the method tends to fail under more complex scenarios as the aerosol stratification within the PBL or the coupling of aerosol layers with the PBL. To improve the PBL height retrieval for these more complex situations, we introduce the use of the depolarization measurements by means of the POLARIS algorithm described in the next section.

3.2Description of POLARIS

POLARIS is based on the detection of the sharp decrease of the aerosol load with height using the range corrected signal and on the relative changes in the aerosol particle shape with height using the perpendicular-to-parallel signal ratio (δ): low δ values might related to spherical particle shape and vice versa (Gross et al., 2011). Since POLARIS is based on vertical relative changes, the depolarization calibration is not required facilitating the procedure. POLARIS uses 10-min averaged range corrected signal (RCS) and perpendicular-to-parallel signal ratio (δ) and carries out the following steps:

1) The WCT is applied to the RCS and to δ (W_{RCS} and W_{δ}, respectively). Then, W_{RCS} (W_{δ}) signal is normalized to the maximum value of RCS (δ) in the first one (two) kilometer(s) above the surface.

2) Three z_{PBL} candidates are determined:

   i) C_{RCS}: the height of the W_{RCS} maximum closest to the surface exceeding a certain threshold η_{RCS} (dimensionless). This threshold is iteratively decreased, starting in 0.05, until C_{RCS} is found (Granados-Muñoz et al., 2012). A dilation value (a_{RCS}) of 0.03 km is used according to Granados-Muñoz et al. (2012).

   ii) C_{min}: the height of the W_{δ} minimum closest to the surface exceeding the threshold η_{min} (dimensionless). This threshold is iteratively increased, starting in -0.05, until C_{min} is found. C_{min} indicates the height of the strongest increase of δ.

   iii) C_{max}: the height of the W_{δ} maximum closest to the surface exceeding the threshold η_{max} (dimensionless). This threshold is iteratively decreased, starting in 0.05, until C_{min} is found. C_{max} indicates the height of the strongest decrease of δ.

3) The z_{PBL} attribution is performed comparing the relative location of the candidates since we have experimentally found that each distribution in height of the candidates (e.g, $C_{max}>C_{min}>C_{RCS}$; $C_{min}>C_{max}>C_{RCS}$) can be linked with an atmospheric situation as schematized in the flow chart (Fig. 3) and explained below:

a. Only one candidate is found: the z_{PBL} corresponds to the found candidate.

b. Only two candidates are found: the z_{PBL} corresponds to the minimum of the found candidates (Fig. 3 case A). An example is shown in Fig. 4 case A.

c. The three candidates are found: in this case, the attribution of the z_{PBL} has two well-differentiated ways:

   c.1. Two matching candidates (~~C_{RCS}~~=C_{max} or C_{RCS}=C_{min}): it is considered that C_{RCS} matches C_{max} or C_{min} when the distance between them is less than 150 m. In these cases, the highest (in altitude) of the matching candidates is discarded, leaving only two candidates. Then, we define two layers: from ~~the full overlap~~ 120 m agl ~~height up~~ up to the lowest candidate, and the layer between ~~from~~ the lowest ~~candidate the lowest layer up to the~~ and the highest candidate. Then, we retrieve the averages ($\bar{\delta}_{C_{RCS}}$ and $\bar{\delta}_{\delta}$ in Fig. 3) and the variances of δ of the both layers. When the absolute difference between the average value of δ is lower than a threshold δ_{Δ} and the variances differ less than 30%, the aerosol type in both layers are considered equal indicating that mixing processes evolve up to the highest candidate. Thus, the z_{PBL} is attributed to the maximum of the two candidates (Fig. 3 and 4 case B or

Mis en forme : Anglais (Royaume-Uni)

D). Conversely, the aerosol types in both layers are considered different indicating that there is not mixing between the layers and thus, the lowest candidate is the z_{PBL} (Fig. 3 and 4 case C or E).

c.2. No match among the candidates: this situation indicates that the sharpest decrease of the RCS does not coincide with the sharpest decrease/increase of the δ.

c.2.1. $C_{max}>C_{min}>C_{RCS}$: this situation is experimentally linked to either an aerosol layer coupled to the PBL (both layers are in contact) or a lofted aerosol layer (aerosol layer above the PBL) within the free troposphere. In the case of aerosol layer coupled to the PBL, C_{max} is the top of the coupled layer (i.e., C_{max} is not the z_{PBL}); C_{min} is the limit between the PBL and the coupled layer; and C_{RCS} is an edge of an internal structure within the PBL. In the case of lofted aerosol layer, C_{max} and C_{min} are the top and the base of a lofted layer, respectively whereas C_{RCS} is the z_{PBL}. To differentiate the two situations, we search a local minimum of the W_{RCS} around C_{min} (i.e., $min\left(W_{RCS}(C_{min} \pm 50\ m)\right)$ larger than η_{RCS}^{min}, dimensionless) since the bottom~~top~~ of a lofted layer would also show an increase of the RCS at the same altitude that δ increases (C_{min}). If found, it is confirmed that C_{min} is the bottom of a lofted layer and thus, the z_{PBL} corresponds to C_{RCS} (Fig. 3 and 4 case F). Otherwise, C_{min} detects the z_{PBL} (Fig. 3 and 4 case G).

c.2.2. $C_{min}>C_{max}>C_{RCS}$: this situation indicates that first RCS decreases, then δ decreases, and finally δ increases. This situation is linked to a multi-layered PBL. In this case, the attribution of the z_{PBL} is performed considering the altitude at which both RCS and δ profiles have the sharpest decrease. To this aim, $\sum_{max}$ and $\sum_{RCS}$ are defined as

$$\sum_{max} = W_{\delta}(C_{max}) + max\left(W_{RCS}(C_{max} \pm 50\ m)\right) \quad \text{Eq. 2}$$

$$\sum_{RCS} = W_{RCS}(C_{RCS}) + max\left(W_{\delta}(C_{RCS} \pm 50\ m)\right) \quad \text{Eq. 3}$$

where $max\left(W_{RCS}(C_{max} \pm 50\ m)\right)$ is the maximum of W_{RCS} in the range $C_{max} \pm 50\ m$ and $max\left(W_{\delta}(C_{RCS} \pm 50\ m)\right)$ is the maximum of W_{δ} in the range $C_{RCS} \pm 50\ m$. Physically, the parameters $\sum_{max}$ and $\sum_{RCS}$ are the sum of the WCT where both RCS and δ profiles have a sharp decrease. Then, if $\sum_{max} > \sum_{RCS}$, both RCS and δ present a ~~at C_{max}~~ stronger at C_{max} than at C_{RCS} and thus, the z_{PBL} is attributed to C_{max} (Fig. 3 and 4 case J), otherwise the z_{PBL} is attributed to C_{RCS} (Fig. 3 and 4 case I).

c.2.3. In the rest of height distributions of C_{min}, C_{max} and C_{RCS} not considered in b.2.1 and b.2.2, the z_{PBL} is attributed to the minimum of the candidates (C_{min} and C_{max}) (e.g., Fig. 3 and 4 case H).

Finally, the temporal coherence of the z_{PBL} is checked ~~using the procedure~~ as proposed by Angelini et al. (2009) and Wang et al. (2012). Once z_{PBL} is determined for a certain period, each z_{PBL} is compared with their previous and subsequent values. Those z_{PBL}^{POL} which differ more than 300 m with respect to their previous and subsequent values are considered unrealistic and thus, replaced by the average value of its three or six previous and latter values if available. In this way we guarantee the smoothness of the temporal series of the z_{PBL}. According to Angelini et al. (2009), occasional aerosol stratification may occur within the mixing layer. This type of stratification which are usually short in time are not really linked with the planetary boundary development leading a false detections of the PBL height. A 7-bin moving median filter is used to reject the possible attributions related to this type of aerosol stratification.

To illustrate how the distribution in height of the candidates is related to a specific atmospheric situation, we analyse a particular case at 21:30 UTC on 16 June 2013 (Fig. 5) corresponding to an example of the c.1 scenario. As can be seen, C_{RCS} and C_{max} are located at 4.46 and 4.41 km agl whereas C_{min} is located at 0.7 km agl. Since the different between C_{RCS} and C_{max} is lower than 0.15 km, we assume that both candidates points to the same edge of the layer and thus, this situation corresponds to $C_{RCS} = C_{max} > C_{min}$. The mean and variance of δ in the layer below C_{min} and the layer between C_{min} and C_{max} are 0.65 and $7{\cdot}10^{-4}$ and 0.99 and $91{\cdot}10^{-4}$, respectively. Since the δ mean difference is larger than δ_t and the variances

Mis en forme ...
Mis en forme ...
Mis en forme : Anglais (Royaume-Uni)
Mis en forme ...
Mis en forme ...
Mis en forme ...
Mis en forme : Anglais (Royaume-Uni)
Mis en forme ...
Mis en forme ...
Mis en forme ...
Mis en forme ...
Mis en forme ...
Mis en forme ...
Mis en forme ...
Mis en forme ...
Mis en forme ...
Mis en forme ...
Mis en forme ...
Mis en forme ...
Mis en forme ...
Mis en forme ...
Mis en forme ...
Mis en forme ...
Mis en forme ...
Mis en forme ...
Mis en forme ...
Mis en forme ...
Mis en forme ...
Mis en forme ...
Mis en forme : Anglais (Royaume-Uni)
Mis en forme ...
Mis en forme : Normal, Sans numérotation ni puces
Mis en forme : Normal
Mis en forme : Exposant
Mis en forme : Couleur de police : Automatique

differ more than 30%, we determine that there are two different layers: the ~~residual layer~~ PBL(z_{PBL}) (low δ) and the coupled layer (high δ) where $C_{RCS} = C_{max}$ indicates the coupled layer top and C_{min} indicates the limit between the residual and the coupled layer, being chosen as z_{PBL}. In this particular case, POLARIS improves the z_{PBL} detection from 4.46 agl to 0.7 km agl.

Mis en forme : Anglais (Royaume-Uni)

3.3 POLARIS adjustment

Fig. 6 shows the time series of the RCS and δ at 532 nm for the 36-hour lidar measurement (10:00 UTC 16 – 19:30 UTC 17 June) of ChArMEx 2013 campaign, the C_{RCS}, C_{max} and C_{min} candidates and the z_{PBL}^{POL} and z_{PBL}^{MWR}. This measurement is used to optimize the algorithm, optimizing the dilation a_δ and the different thresholds (η_{RCS}^{min}, and δ_t). ~~F~~Following a similar procedure as that explained in Granados-Muñoz et al. (2012), different combinations of dilation and threshold values are used to compute z_{PBL}^{POL}. ~~the tracers are different and the weakness of the PBL detection using a microwave radiometer (z_{PBL}^{MWR}) already aforementioned in Section 2. We just use z_{PBL}^{MWR} as an illustrative of the PBL top location to adjust and validate POLARIS since it is unique alternative available during the campaign.~~

Low dilation values (e.g., <0.2 km) provide wrong PBL detection since the WCT identifies as edge changes in the signal that are related to the noise of the δ profile whereas. ~~lL~~arge dilation values (e.g., >0.5 km) detect only strong edges (e.g., the top of the dust layer). ~~Despite even with a larger dilation the PBL height is detected in some case, the PBL height is discarded when the transition is weak like those cases when the PBL is coupled with the dust layer.~~ The~~Optimal~~ optimal dilation (a_δ) ~~for the depolarization profile a_δ~~ is established at ~~450 m~~0.45 km. This a_δ value ~~which~~ is larger than the ~~a_{RCS}~~ dilation for the RCS profile ~~300 m~~(0.3 km) determined by Granados-Muñoz et al. (2012) which may be due to the fact ~~the~~ δ ~~used to be~~ is noisier than ~~the~~ RCS. ~~and thus, it~~~~The~~.In the case of η_{RCS}^{min}, the threshold used to distinguish decoupled layers, a value of 0.01 ~~is~~ is chosen considering the signal-to-noise ratio of the RCS in the firsts kilometer of the atmospheric column. A δ_t value (used in the case b.1 for distinguishing two aerosol layers) ~~is~~ of 0.06~~.~~ is determined since ~~L~~lower values ~~would~~ separate the same aerosol layer ~~that only present~~ with slight internal variations and larger values ~~would~~ difficult the ~~distinction~~differentiation between the mixing and residual layer with similar δ values.

During this optimization process z_{PBL}^{MWR} is used as reference. The goal is to minimize the differences between z_{PBL}^{MWR} and z_{PBL}^{POL}, even though discrepancies are still expected between both methodologies due to the use of different tracers (temperature for the MWR and aerosol for POLARIS) and the uncertainties associated to both methods.

~~according to the results obtained in the optimization process.~~The z_{PBPBL}^{POL} determined with the optimal values of a_δ, η_{RCS}^{min}, and δ_t is shown in Fig. 6.

During night-time (from 20:30 UTC on 16 June to 04:00 UTC 17 June), we compare the residual layer height determined by the method which uses only the RCS (C_{RCS}) and by POLARIS (z_{PBRL}^{POL}) and the stable layer height determined with the MWR (z_{PBSL}^{MWR}). The C_{RCS} candidates are mainly pointing to ~~almost does not detect the edges between the~~ either the top of the ~~PBL~~ dust layer or ~~and the different stratifications within~~ internal substructures within the dust layer (Fig. 6)~~, overlaying the PBL~~. However, POLARIS distinguishes the transition between the residual aerosol layer and the dust layer. In addition, C_{RCS} shows no or little temporal coherency and large discrepancies with z_{SL}^{MWR} as it is evidenced by the means and standard deviations of the C_{RCS} (2.42±1.6 km agl) and of z_{PBSL}^{MWR} (0.22±0.01~~1.6~~ km agl). On the contrary, z_{RL}^{POL} (0.82±0.3 km agl) is more stable with time than C_{RCS} with closer values to z_{SL}^{MWR}, providing more reliable results. The offset of 6405~~0~~ m observed between z_{SL}^{MWR} and z_{RL}^{POL} during the night is mostly due to the fact that z_{RL}^{POL} corresponds to the residual layer and z_{RL}^{MWR} marks the top of the nocturnal stable layer.

On 16 June 2013, the mean and standard deviation of z_{PBML}^{POL}, z_{PBML}^{MWR} and C_{RCS} during daytime ~~is~~ are ~~3.4±0.4~~2.0±0.3, 2.7±0.4 ~~2.7±0.3~~ and ~~2.2~~1.5±1.1 km a~~s~~gl, respectively. C_{RCS} mean is more than 1 km lower than z_{PBML}^{MWR} because C_{RCS} ~~indicates layering~~is

~~points~~ most frequently detecting internal structures rather than the top of the PBL. The large standard deviation of the C_{RCS} (1.1 km) is caused by the detections of either the structures within the PBL at around 1.~~8~~ 12 km agl or the top of the dust layer at around ~~4.5~~3.8 km ~~asl~~ agl (Fig. 6). On the contrary, z_{PBML}^{POL} mean provides a more comparable value with similar standard deviation. These results evidence that the method which uses only the RCS fails when a dust layer is overlaying the PBL. Besides, z_{PBML}^{POL} fits better the trend of ~~and~~ z_{PBML}^{MWR}~~, is, in general, very similar although the z_{PBL}^{POL} values are lower than the z_{PBL}^{MWR} ones.~~

The main differences between z_{MPBL}^{POL} and z_{MPBL}^{MWR} are caused by the different basis of each methodology: z_{MPBL}^{MWR} is determined using the temperature as tracer whereas POLARIS uses the aerosol. For example, on 16 June 2013, z_{MPBL}^{MWR} increases from 0.8 km to 2.02 km agl between 10:15 and 11:30 UTC whereas z_{MPBL}^{POL} increases abruptly from 0.52 to 1.82 km agl between 11:20 and 11:30 UTC (i.e., almost one hour later). This is because z_{MPBL}^{MWR} growths due to the increase of the temperature at surface level during the morning whereas z_{MPBL}^{POL} increases later, once the convection processes are strong enough to dissipate the boundary between the mixing and the residual layer. Another example of the influence of the tracer is the 1-km bias between z_{MPBL}^{POL} and z_{MPBL}^{MWR} between 18:00 and 21:00 UTC on 16 June 2013. During the late afternoon and early night, the temperature at surface level quickly decreases and the atmospheric stability suddenly changes from instable to stable. This pattern is registered by the z_{MPBL}^{MWR} decreasing from 1.82 km to 0.055 km agl between 18:00 and 18:30 UTC. The increasing atmospheric stability during the late afternoon and early night stops the convection processes and then the mixing layer becomes the residual layer. This change from mixing to residual layer is tracked by the temporal evolution of z_{RPBL}^{POL} decreasing from 1.92 km to 0.52 km agl between 18:00 and 24:00 UTC. Therefore, there are differences between z_{PBLPBL}^{POL} and z_{PBPBL}^{MWR} explained in terms of the tracer used for each method that are not related to a wrong attribution of POLARIS.

~~Also, a delay of the z_{PBL}^{POL} increase z_{PBL}^{POL} with respect to the z_{PBL}^{MWR} increase z_{PBL}^{MWR} during the transition from the residual layer to the mixing one. For example, z_{PBL}^{POL} increases abruptly from 1200 1.2 to 2500 2.5 km asl between 11:20 and 11:30 UTC whereas z_{PBL}^{MWR} increases from 1.48 km to 2.7 km between 10:15 and 11:30 UTC (i.e., almost one hour delay). These discrepancies could not be fixed during the optimization process due to their different basis: z_{PBL}^{MWR} method uses thermodynamic variables as tracer whereas POLARIS uses the aerosol. Therefore, z_{PBL}^{MWR} increases with the development of the convective processes but the vanishing of the residual layer edge (aerosol as tracer) only occur once the convection processes are strong enough. Besides discrepancies, both z_{PBL}^{POL} and z_{PBL}^{MWR}, with low standard deviations, show comparable temporal evolution indicating the goodness of the method and thus, POLARIS also improves the z_{PBL} detection during daytime.~~

4 Validation of POLARIS

Mis en forme : Anglais (Royaume-Uni)

After the optimization process, POLARIS is applied in an automatic and unsupervised way to the 72-hour lidar measurement performed during the ChArMEx 2012 campaign (between 9 and 12 July 2012). POLARIS is evaluated comparing z_{PBL}^{POL}, with z_{PBL}^{MWR} and C_{RCS}~~z_{PBL}^{RCS}~~. During this campaign, a Saharan dust outbreak occurred over the Southern Iberian Peninsula. As it can be seen in Fig. 7, δ values are lower close to the surface (mainly local anthropogenic aerosols) in comparison with the lofted aerosol layers (dust aerosol plumes).

The detection of the z_{PBL} by means of the method applied by Granados-Muñoz et al. (2012) (C_{RCS}) shows an erratic trend during the analysed period when the dust layer is coupled to the PBL (Fig. 7). As it can be seen, C_{RCS} sometimes detects either the top of the dust layer, as in the periods 19:30-22:00 UTC on 09/07 and 15:40-16:10 UTC on 11/07 reaching values above 5

km agl or an internal structure within the dust layer (e.g., between 11:50 and 12:20 UTC on 11/07). These estimations are really far from the z_{ML}^{MWR} and thus, they are not linked with the top of the mixing layer. For example, in the period 15:40-16:10 UTC on 11/07, the difference between C_{RCS} and z_{ML}^{MWR} is around 3 km whereas the difference between z_{ML}^{POL} and z_{ML}^{MWR} is around 0.5 km and thus, we can conclude that the estimation performed using POLARIS significantly improves the detection of the z_{PBL} when an aerosol layer is coupled to the PBL. ~~However, comparison POLARIS y CRCS durante el día y la noche. Se ve la diferencia enorme entre ambos. Y como POLARIS es mejor, JODER.~~

POLARIS and the method applied by Granados-Muñoz et al. (2012) (C_{RCS}) agree with discrepancies lower than 250 m when the dust layer is decoupled of the PBL (e.g., 00:00-08:00 UTC 10 July, 00:00-09:00 UTC 11 July and 18:00 11 July - 04:45 UTC 12 July). ~~Therefore~~ evidencing that the use of ~~,~~ POLARIS ~~algorithms~~ is also appropriate when no coupled layers are present. ~~However, comparison POLARIS y CRCS durante el día y la noche. Se ve la diferencia enorme entre ambos. Y como POLARIS es mejor, JODER.~~

~~Furthermore, the comparison between z_{PBL}^{POL} and z_{PBL}^{MWR} revealed showed that the detection of the z_{PBL} becomes particularly difficult when the mixing is ongoing (07:00-13:00 GMT) coexisting the residual and mixing layer. As it can be seen in Fig. 7 from 07:00 until 13:00 UTC on 11 July, z_{PBL}^{MWR} is increasing (mixing layer is growing) whereas z_{PBL}^{POL} is decreasing from 07:00 until 12:20 UTC (subsidence of the residual layer). During this period, despite the MWR points to convective processes, δ shows a layered structure. Therefore, the convective processes already initiated does not produces the necessary mixing that leads to the suppression of the residual layer. In fact, according to the δ edges provided by POLARIS (red and yellow triangles, Fig. 8), the mixture is almost complete around 13:15 UTC.~~

~~POLARIS and the method applied by Granados-Muñoz et al. (2012) (C_{RCS}) agree with discrepancies lower than 250 m when the dust layer is decoupled of the PBL (e.g., 00:00-08:00 UTC 10 July, 00:00-09:00 UTC 11 July and 18:00 11 July - 04:45 UTC 12 July). Therefore, the use of δ profiles~~POLARIS ~~algorithms is also appropriate without coupled layers.~~

The comparison between z_{PBML}^{POL} and z_{PBML}^{MWR} shows a good agreement when the mixing layer is well developed (13:00-16:00 UTC on each day). However, some discrepancies are found (e.g., 14:46 UTC 10 July 2012 and 15:51 UTC 11 July 2012). These differences can be easily explained considering the different uncertainties and tracers of both methods, which have different responses during the changing conditions, e.g. those observed during sunset or sunrise. During night-time (e.g. 20 UTC 9 July), the offset between the residual and stable layer can be easily tracked with ~~due to the POLARIS detection of the residual layer whereas the z_{PBL}^{MWR} indicates the stable layer between 100 and 300 m above ground level~~ z_{PBRL}^{POL} and z_{PBSL}^{MWR}. POLARIS detects the residual layer instead of the stable layer because the WCT can ~~, the overlap region cannot be completely corrected~~ be applied only from $a_\delta/2$ meters above the first valid value of the profile (~0.25 km agl), i.e., around ~450 m, whereas the z_{SL}^{MWR} is between 100 and 300 m agl ~~the residual layer top will be detected instead of the stable layer when the stable layer is below the overlap height of the δ profiles~~.

5. WRF validation using POLARIS and MWR

Mis en forme : Anglais (Royaume-Uni)

Recent studies use the z_{PBL} determined using lidar data to validate the z_{PBL} obtained from WRF model (z_{PBL}^{WRF}) (Xie et al., 2012; Pichelli et al., 2014 and Banks et al., 2015). In this section, we take the advantage of the z_{PBL} determined by POLARIS (z_{PBL}^{POL}) together with the microwave radiometer z_{PBL}^{MWR} during CHArMEx 2012 and 2013 to validate the z_{PBL}^{WRF}.

5.1 WRF model setup

Mis en forme : Anglais (Royaume-Uni)

~~The WRF NWP model, version 3.6.1, was used to analyse the CHARMEX 2012 and 2013 campaigns.~~ The model configuration consists of four nested domains with 27, 9, 3 and 1 km (approximately) spatial resolution domains, respectively, and 50 vertical levels. The outputs (i.e., temperature, wind, and humidity profiles, etc.) of the 1-km domain are analysed. The initial and

boundary conditions for the WRF model runs are taken from the NCEP High Resolution Global Forecast System data set (www.emc.ncep.noaa.gov) every 6 hours. ~~The 1-km WRF outputs are saved every 5 minutes.~~

The choice of the model physical parameterization is based on the results of previous evaluation studies conducted in the study area (Arbizu-Barrena et al., 2015 ~~Santos-Alamillos et al., 2013~~). Particularly, the Mellor-Yamada Nakanishi and Niino Level 2.5 is selected for the PBL parameterization (Nakanishi and Niino, 2009)~~. This parameterization performs Turbulent Kinetic Energy advection and accounts for both sensible and latent heat fluxes as well as moisture flux from the surface~~. The parameterizations used for the rest of physical schemes are: the Eta (Ferrier) microphysics parameterization scheme (Rogers et al., 2005), the RRTM long-wave radiation parameterization (Mlawer et al., 1997), the Dudhia scheme for short-wave radiation parameterization (Dudhia, 1989), the 5-layer thermal diffusion land surface parameterization (Dudhia, 1996) and, for coarser domains, the Kain-Fritsch (new Eta) cumulus parameterization (Kain, 2004).

5.2 Comparison of the PBL heights determined by WRF, POLARIS and microwave radiometer

Fig. 6 and 7 show the temporal evolution of the PBL heights determined by means of POLARIS (z_{PBL}^{POL}), the MWR (z_{PBL}^{MWR}) and WRF~~, z_{PBL}^{POL}, z_{PBL}^{MWR}, and~~ (z_{PBL}^{WRF},)~~respectively. The period represent accounts for the RCS and δ at 532 nm~~ during the ChArMEx campaign on 2012 (09:00 UTC 16 June– 20:00 UTC 17 June) and 2013 (12:00 UTC 9 July – 06:00 12 July).

During daytime on both campaigns, WRF underestimates the z_{PBL} (lower values) with respect to z_{PBL}^{POL} and z_{PBL}^{MWR} in agreement with the study presented by Banks et al. (2015) and Banks and Baldasano (2016). For example, z_{PBL}^{WRF} is 1 km below z_{PBL}^{POL} and z_{PBL}^{MWR} on 16/06 2013 (Fig. 6) and on 9 and 10 July 2012 (Fig. 7). Nevertheless, the z_{PBL} time series of all methods show similar patterns. Table 1 shows the determination coefficient R^2 and the mean of the differences (i.e., bias) among z_{PBL}^{WRF}, z_{PBL}^{POL} and z_{PBL}^{MWR} during night- and day-time.

During free-cloud day-time, the correlation between z_{PBL}^{WRF} and z_{PBL}^{POL} can be well differentiated. $R_{POL-WRF}^2$ is larger on 10 and 11 July 2012 than on 9 July 2012 and 16 June 2013. According to the time series of the δ (Fig. 6 and 7), it can be seen that the coupling of the dust layer to the PBL is stronger on 10 and 11 July 2012 than on 9 July 2012 and 16 June 2013. Additionally, the mean of bias values between POLARIS and WRF ($\overline{\Delta_{PBL}^{POL-WRF}}$), larger than 800 meters, points to the aforementioned underestimation of the convective processes. At this regard, several possibilities are feasible: (i) too stringent conditions for the WRF parameterization, which can influence directly the results (Xie et al., 2012; Banks et al., 2015); (ii) insufficient number of the WRF model vertical levels within the PBL limits; (iii) the different definitions of the PBL applied to each method, and (iv) the presence of Saharan dust layer (Fig. 6 and 7). Among these causes, the (i) and (ii) should affect to the whole period, not only the periods with the strongest coupling of the dust layer to the PBL. In addition, the different definitions of PBL seem difficult to give rise to such a large bias. In fact, POLARIS and the parcel method use different tracers (e.g., temperature~~, MWR,~~ and aerosol~~, POLARIS~~) but they generally show better agreement than WRF. Thus, the more plausible cause is the inability of the used WRF PBL parameterization to account properly for this particular kind of events.

The correlations between MWR and WRF ($R_{MWR-WRF}^2$) are between 0.395 and 0.664 during free-cloud day-time without a clear dependence with the presence or the coupling of the dust layer. The lowest $R_{MWR-WRF}^2$ and the largest $\overline{\Delta_{PBL}^{MWR-WRF}}$ ocurs ~~The lowest correlations between POLARIS and WRF occur on 16 and 17 June 2013.~~ on 16 June in coincidence with the lowest $R_{POL-WRF}^2$. On this day, ~~The~~ the WRF model estimates that the convective processes ~~is~~ start at 13:35 and ends at 16:15 UTC, ~~for the WRF model~~ whereas ~~the~~ MWR detects convective processes between ~~10h30~~ 10:30 and ~~18h00~~ 18:00 UTC (i.e., 5 hours difference). The good agreement between POLARIS and MWR ($R_{POL-MWR}^2$ = 0.803) indicates that the main cause of the differences in the PBL height is the short duration of the convective processes estimated by the WRF model.

During night-time, z_{PBL}^{WRF} and z_{PBL}^{MWR} agree, with differences below ~~200~~0.238 km (see Table 1). However, ~~and even being the same during some periods (e.g., from 01:52 to 05:11 UTC on 10 July 2012, see Fig. 8) whereas~~ a ~~almost~~ low temporal correlation is observed (~~with $\overline{\Delta_{PBL}^{MWR-WRF}}$~~ $R_{MWR-WRF}^2$ values between 0.032 and 0.364), showing the opposite behaviour

observed during daytime. The large ~~bias~~ $\overline{\Delta_{PBL}^{POL-WRF}}$ and $\overline{\Delta_{PBL}^{POL-MWR}}$ values evidence ~~that the~~ that POLARIS detects the residual layer whereas~~stable layer height is generally too low to be detected by POLARIS, and thus, POLARIS provides the top of the residual layer~~ MWR and WRF detect the top of the stable layer. ~~Note that~~Despite POLARIS and WRF are detecting different layers, we find a larger correlation~~, overall,~~ among them (~~the~~ $R^2_{POL-WRF}$ ~~,~~) than between MWR and WRF (~~and~~ $R^2_{MWR-WRF}$~~)values point to a more similar behaviour between POLARIS and WFR than between MWR and WRF~~.

Finally, the lowest $R^2_{POL-WRF}$ coincides with the lowest $\overline{\Delta_{PBL}^{POL-WRF}}$ and $\overline{\Delta_{PBL}^{MWR-WRF}}$ values on 17 June. The presence of clouds from midday (cloud base at ~~10~~ 9.32 km ~~asl~~agl) until the end of the measurements (cloud base at ~~2~~1.32 km a~~s~~gl) may explain this behaviour since i) the systematic underestimation from WRF might be compensated by the cloudy conditions inhibiting the strength of convective processes and ii) the track of the PBL evolution is more difficult to fit during cloudy conditions, considering the different tracers (i.e., aerosol and temperature).

To sum up, ~~D~~during night-time, z_{PBL}^{WRF} and z_{PBL}^{MWR} values agree but more similar temporal evolution is found between WRF and POLARIS~~:~~. ~~during~~ However, during daytime, the WRF model underestimates the z_{PBL}. Since POLARIS allows detecting reliable PBL heights under Saharan dust outbreaks, it might be used for the improvement of the WRF parameterization. ~~During night-time, values reported by the WRF closely agree with the experimental MWR z_{PBL} values.~~

6. Conclusion

The perpendicular-to-parallel signal ratio (i.e., the uncalibrated volume linear depolarization ratio), together with the lidar range corrected signal, are used to develop a new algorithm, called POLARIS, for the detection of the planetary boundary layer height (z_{PBL}). The z_{PBL} provided by POLARIS, z_{PBL}^{POL}, is optimized by comparison with the z_{PBL} derived from microwave radiometer measurements (temperature profiles), z_{PBL}^{MWR}, using continuous 36-hour lidar and MWR measurements. z_{PBL}^{POL} is validated by comparison with the z_{PBL}^{MWR}, using continuous 72-hour lidar and MWR measurements. These measurements were performed during the ChArMEx campaigns conducted in 2012 and 2013. These ~~long~~continuous-term measurements are crucial for the adjustment and validation of POLARIS since they allow the tracking of the evolution of the coupling between advected aerosol layers and the planetary boundary layer. A ~~good~~ better agreement is obtained between POLARIS and the methods applied to the MWR measurements compared with the WCT method exclusively applied to the range corrected signal during complex scenarios (e.g., ~~even~~ when a Saharan dust layer is coupled to the PBL). Despite POLARIS is validated using dust layers coupled to the PBL, a priori, it can be used for any layer coupled to the PBL if the aerosol particle-shape is different enough to be detected by the depolarization profile. This is a remarkable improvement compared to previous methods based on the WCT applied to the RCS.

The z_{PBL} is also determined by means of WRF model, z_{PBL}^{WRF}, under Saharan dust outbreaks. During daytime, z_{PBML}^{WRF} is considerably lower than z_{PBML}^{POL} and z_{PBML}^{MWR} with larger differences under coupling-layer situation. However, WRF and MWR provides similar z_{PBL} during night-time although z_{PBSL}^{WRF} shows a better temporal correlation with z_{PBRL}^{POL} than with z_{PBSL}^{MWR}. The comparison between POLARIS and WRF evidences the model difficulties to determine the z_{PBL} when advected layers are coupled to the PBL. Since POLARIS allows the detection of reliable PBL heights under Saharan ~~Therefore,~~ dust outbreaks, it might be used for the improvement of the WRF parametrization.

~~POLARIS~~ This study ~~tools been~~ demonstrates that the depolarization measurement is an interesting proxy for the PBL detection since ~~allows a better model validation since~~ it provides ~~confident~~ reliable PBL heights ~~event~~ under coupling-layer situation~~complex atmospheric situations~~. Moreover, considering the next ceilometer generations with depolarization capabilities, ~~POLARIS~~ this study will be useful for an automatic and unsupervised PBL detection. At this regard, further investigations ~~would~~ will lead to a proper PBL height detection in all atmospheric conditions.

Acknowledgements

This work was supported by the Andalusia Regional Government through project P12-RNM-2409, by the Spanish Ministry of Economy and Competitiveness through projects CGL2013-45410-R and CGL2016-81092-R, and by the European Union's Horizon 2020 research and innovation programme through project ACTRIS-2 (grant agreement No 654109). The authors thankfully acknowledge the FEDER program for the instrumentation used in this work. This work was also partially funded by the University of Granada through the contract "Plan Propio. Programa 9. Convocatoria 2013". The authors express gratitude to the ChArMEx project of the MISTRALS (Mediterranean Integrated Studies at Regional and Local Scales; http://www.mistrals-home.org) multidisciplinary research programme.

References

Angelini, F., Barnaba, F., Landi, T. C., Caporaso, L., and Gobbi, G. P.: Study of atmospheric aerosols and mixing layer by lidar, Radiat. Prot. Dosim., 137(3-4), 275-279, doi: 10.1093/rpd/ncp219, 2009.

Arbizu-Barrena, C., Pozo-Vázquez, D., Ruiz-Arias, J. A., and Tovar-Pescador, J.: Macroscopic cloud properties in the WRF NWP model: An assessment using sky camera and ceilometer data. Journal of Geophysical Research: Atmospheres 120 (19), doi: 10.1002/2015JD023502, 2015.

Baars, H., Ansmann, A., Engelmann, R., and Althausen, D.: Continuous monitoring of the boundary-layer top with lidar. Atmospheric Chemistry and Physics, 8, 7281–7296, doi 10.5194/acp-8-7281-2008, 2008.

Banks, R. F., Tiana-Alsina, J., Rocadenbosch, F., and Baldasano, J. M.: Performance evaluation of the boundary-Layer height from lidar and the Weather Research and Forecasting model at an urban coastal site in the North-East Iberian Peninsula,Boundary-Layer Meteorology, 157(2), 265–292, doi: 10.1007/s10546-015-0056-2, 2015.

Banks, R. F., and Baldasano, J. M.: Impact of WRF model PBL schemes on air quality simulations over Catalonia, Spain. Science of the Total Environment 572 (2016) 98–113, doi:10.1016/j.scitotenv.2016.07.167, 2016.

Borge, R., Alexandrov, V., Vas, J. J. del, Lumbreras, J., and Rodríguez, E.: A comprehensive sensitivity analysis of the WRF model for air quality applications over the Iberian Peninsula. Atmos Environ 42(37), 8560–8574, doi: 10.1016/j.atmosenv.2008.08.032,2008.

Bravo-Aranda, J.A, Navas-Guzmán, F., Guerrero-Rascado, J.L., Pérez-Ramírez, D., Granados-Muñoz, M.J., and Alados-Arboledas, L.: Analysis of lidar depolarization calibration procedure and application to the atmospheric aerosol characterization, International Journal of Remote Sensing 34(9-10), 3543-3560, doi: 10.1080/01431161.2012.716546, 2013.

Bravo-Aranda, J. A., Belegante, L., Freudenthaler, V., Alados-Arboledas, L., Nicolae, D., Granados-Muñoz, M. J., Guerrero-Rascado, J. L., Amodeo, A., D'Amico, G., Engelmann, R., Pappalardo, G., Kokkalis, P., Mamouri, R., Papayannis, A., Navas-Guzmán, F., Olmo, F. J., Wandinger, U., Amato, F., and Haeffelin, M.: Assessment of lidar depolarization uncertainty by means of a polarimetric lidar simulator, Atmos. Meas. Tech., 9, 4935-4953, doi:10.5194/amt-9-4935-2016, 2016.

Cairo, F., Di Donfrancesco, G., Adriani, A., Pulvirenti, L., and Fierli F.: Comparison of various linear depolarization parameters measured by lidar, Appl Optics, 38, 4425-4432, doi: 10.1364/AO.38.0044251999.

Collaud-Coen, M. C., Praz, C., Haefele, A., Ruffieux, D., Kaufmann, P., and Calpini, B.: Determination and climatology of the planetary boundary layer height above the Swiss plateau by in situ and remote sensing measurements as well as by the COSMO-2 model. Atmospheric Chemistry and Physics, 14, 13205–13221, doi: 10.5194/acp-14-13205-2014, 2014.

Comerón, A., Sicard, M., and Rocadenbosch, F.: Wavelet correlation transform method and gradient method to determine aerosol layering from lidar returns: Some comments. Journal of Atmospheric and Oceanic Technology, 30(6), 1189–1193, doi: 10.1175/JTECH-D-12-00233.1, 2013.

Mis en forme : Normal

Mis en forme : Police par défaut

Mis en forme

Dandou, A., Tombrou, M., Schäfer, K., Emeis, S., Protonotariou, A., Bossioli, D., Soulakellis, N., and Suppan, P.: A Comparison Between Modelled and Measured Mixing-Layer Height Over Munich. Boundary-Layer Meteorol 131:425–440, doi: 10.1007/s10546-009-9373-7, 2009.

Dudhia, J., 1989: Numerical study of convection observed during the Winter Monsoon Experiment using a mesoscale two–dimensional model. J. Atmos. Sci., 46, 3077–3107, doi: 10.1175/1520-0469(1989)046<3077:NSOCOD>2.0.CO;2, 1988.

Dudhia, J., 1996: A multi-layer soil temperature model for MM5. The Sixth PSU/NCAR Mesoscale Model Users' Workshop. Bouilder, CO.

Dulac, F.: An overview of the Chemistry-Aerosol Mediterranean Experiment (ChArMEx), European Geosciences Union General Assembly, Geophysical Research Abstracts Vol. 16, EGU2014-11441, 27 April–2 May 2014, Vienna, Austria, 2014.

Granados-Muñoz, M. J., Navas-Guzmán, F., Bravo-Aranda, J. A., Guerrero-Rascado, J. L., Lyamani, H., Fernández-Gálvez, J., and Alados-Arboledas, L.: Automatic determination of the planetary boundary layer height using lidar: One-year analysis over southeastern Spain. Journal of Geophysical Research: Atmospheres, 117(D18), doi: 10.1029/2012JD017524, 2012.

Granados-Muñoz, M. J., Navas-Guzmán, F., Guerrero-Rascado, J. L., Bravo-Aranda, J. A., Binietoglou, I., Pereira, S. N., Basart, S., Baldasano, J. M., Belegante, L., Chaikovsky, A., Comerón, A., D'Amico, G., Dubovik, O., Ilic, L., Kokkalis, P., Muñoz-Porcar, C., Nickovic, S., Nicolae, D., Olmo, F. J., Papayannis, A., Pappalardo, G., Rodríguez, A., Schepanski, K., Sicard, M., Vukovic, A., Wandinger, U., Dulac, F., and Alados-Arboledas, L.: Profiling of aerosol microphysical properties at several EARLINET/AERONET sites during the July 2012 ChArMEx/EMEP campaign, Atmos. Chem. Phys., 16, 7043-7066, doi:10.5194/acp-16-7043-2016, 2016.

Gross, S., Tesche, M., Freudenthaler, V., Toledano, C., Weigner, M., Ansmann, A., Althausen, D., Seefeldner, M.: Characterization of Saharan dust, marine aerosols and mixtures of biomass-burning aerosols and dust by means of multi-wavelength depolarization and Raman lidar measurements during SAMUM 2. Tellus B, v. 63B, 706–724, doi:10.3402/tellusb.v63i4.16369, 2011.

Guerrero-Rascado, J. L., Ruiz, B., and Alados-Arboledas, L.: Multi-spectral lidar characterization of the vertical structure of Saharan dust aerosol over southern Spain, Atmos. Envion., 42, 2668-2681, doi:10.1016/j.atmosenv.2007.12.062, 2008.

Guerrero-Rascado, J. L., Olmo, F. J., Avilés-Rodríguez, I., Navas-Guzmán, F., Pérez-Ramírez, D., Lyamani, H., and Alados-Arboledas, L.; Extreme Saharan dust event over the southern Iberian Peninsula in September 2007: active and passive remote sensing from surface and satellite, Atmos. Chem. Phys., 9, 8453-8469, doi: 10.5194/acp-9-8453-2009, 2009.

Helmis, C., Tombrou, M., Schäfe., K., Münkel, C., Bossioli, E. & Dandou, A. : A comparative study and evaluation of mixing-height estimation based on Sodar-RASS, ceilometer data and numerical model simulations, Boundary-Layer Meteorology, 145, 507–526, doi: 10.1007/s10546-012-9743-4, 2012.

Holzworth, G. C.: Estimates of mean maximum mixing depths in the contiguous United States. Monthly Weather Review, 92, 235–242, 10.1175/1520-0493(1964)092<0235:EOMMMD>2.3.CO;2, 1964.

Kain, John S., 2004: The Kain–Fritsch convective parameterization: An update. J. Appl. Meteor., 43, 170–181, doi: http://dx.doi.org/10.1175/1520-0450(2004)043<0170:TKCPAU>2.0.CO;2, 2004.

Lyamani, H., Olmo, F. J., & Alados-Arboledas, L. (2010). Physical and optical properties of aerosols over an urban location in Spain: seasonal and diurnal variability. Atmospheric Chemistry and Physics, 10, 239–254, doi: 10.5194/acp-10-239-2010, 2010.

Mallet, M., Dulac, F., Formenti, P., Nabat, P., Sciare, J., Roberts, G., Pelon, J., Ancellet, G., Tanré, D., Parol, F., Denjean, C., Brogniez, G., di Sarra, A., Alados-Arboledas, L., Arndt, J., Auriol, F., Blarel, L., Bourrianne, T., Chazette, P., Chevaillier, S., Claeys, M., D'Anna, B., Derimian, Y., Desboeufs, K., Di Iorio, T., Doussin, J.-F., Durand, P., Féron, A., Freney, E., Gaimoz, C., Goloub, P., Gómez-Amo, J. L., Granados-Muñoz, M. J., Grand, N., Hamonou, E., Jankowiak, I., Jeannot, M., Léon, J.-F., Maillé, M., Mailler, S., Meloni, D., Menut, L., Momboisse, G., Nicolas, J., Podvin, T., Pont, V., Rea, G., Renard, J.-B., Roblou, L., Schepanski, K., Schwarzenboeck, A., Sellegri, K., Sicard, M., Solmon, F., Somot, S., Torres, B., Totems, J., Triquet, S.,

Mis en forme : Anglais (Royaume-Uni)

Mis en forme : Anglais (Royaume-Uni)

Code de champ modifié

Mis en forme : Anglais (Royaume-Uni)

Verdier, N., Verwaerde, C., Waquet, F., Wenger, J., and Zapf, P.: Overview of the Chemistry-Aerosol Mediterranean Experiment/Aerosol Direct Radiative Forcing on the Mediterranean Climate (ChArMEx/ADRIMED) summer 2013 campaign, Atmos. Chem. Phys., 16, 455-504, doi:10.5194/acp-16-455-2016, 2016.

Meunier, V., Löhnert, U., Kollias, P., and Crewell, S.: Biases caused by the instrument bandwidth and beam width on simulated brightness temperature measurements from scanning microwave radiometers, Atmospheric Measurement Techniques, 6, 1171–1187, doi:10.5194/amt-6-1171-2013,2013.

Milovac, J., Warrach-Sagi, K., Behrendt, A., Späth, F., Ingwersen, J., and Wulfmeyer, V.: Investigation of PBL schemes combining the WRF model simulations with scanning water vapor differential absorption lidar measurements, J. Geophys. Res. Atmos., 121, 624–649, doi:10.1002/2015JD023927, 2016.

Morille, Y., Haeffelin, M., Drobinski, P., and Pelon, J.:STRAT: An Automated Algorithm to Retrieve the Vertical Structure of the Atmosphere from Single-Channel Lidar Data. Journal of Atmospheric and Oceanic Technology, 24(5), 761–775, doi: 10.1175/JTECH2008.1, 2007.

Mlawer, E. J., Taubman, S. J., Brown, P. D., Iacono, M. J., and Clough, S. A.: Radiative transfer for inhomogeneous atmospheres: RRTM, a validated correlated–k model for the longwave. J. Geophys. Res.,102, 16663–16682, doi: 10.1029/97JD00237, 1997.

Nakanishi, M., and Niino, H.: Development of an improved turbulence closure model for the atmospheric boundary layer. J. Meteor. Soc. Japan, 87, 895–912, doi: 10.1029/97JD00237, 2009.

Navas Guzmán, F., Guerrero Rascado, J. L., and Alados Arboledas, L.: Retrieval of the lidar overlap function using Raman signals, Óptica Pura y Aplicada, 44(1), 71-75, 2011.

Navas-Guzmán, F., Fernández-Gálvez, J., Granados-Muñoz, M. J., Guerrero-Rascado, J. L., Bravo-Aranda, J. A., and Alados-Arboledas, L. (2014). Tropospheric water vapour and relative humidity profiles from lidar and microwave radiometry. Atmospheric Measurement Techniques, 7(5), 1201–1211, doi: 10.5194/amt-7-1201-2014, 2014.

Pal, S., Behrendt, A., and Wulfmeyer, V.: Elastic-backscatter-lidar-based characterization of the convective boundary layer and investigation of related statistics. Annales Geophysicae, 28(3), 825–847, doi: 10.5194/angeo-28-825-2010, 2010.

Pichelli, E., Ferretti, R., Cacciani, M., Siani, A. M., Ciardini, V., and Di Iorio, T.:The role of urban boundary layer investigated with high-resolution models and ground-based observations in Rome area: A step towards understanding parameterization potentialities. Atmospheric Measurement Techniques, 7(1), 315–332, doi: 10.5194/amt-7-315-2014, 2014.

Rogelj, N., Guerrero-Rascado, Navas-Guzmán, F., Bravo-Aranda, J. A., Granados-Muñoz, M. J., Alados-Arboledas L.: Experimental determination of UV- and VIS- lidar overlap function. Optica Pura Y Aplicada, 47, 169-175, doi: 10.7149/OPA.47.3.169, 2011.

Rogers, E., Black, T., Ferrier, B., Lin, Y., Parrish, D., and DiegoG.: Changes to the NCEP MesoEta Analysis and Forecast System: Increase in resolution, new cloud microphysics, modified precipitation assimilation, modified 3DVAR Analysis. Available online at www.emc.ncep.noaa.gov/mmb/mmbpll/eta12tpb/), 2005.

Rose, T., Crewell, S., Lohnert, U., and Simmer C.: A network suitable microwave radiometer for operational monitoring of the cloudy atmosphere, Atmos Res, 75(3), 183-200, doi: 10.1016/j.atmosres.2004.12.005, 2005.

~~Santos-Alamillos, F., Pozo-Vázquez D., Ruiz-Arias, J.A., Lara-Fanego, V. and Tovar-Pescador, J.: Analysis of WRF model wind estimate sensitivity to physics parameterization choice and terrain representation in Andalusia (Southern Spain). Journal of Applied Meteorology and Climatology 52 (7), 1592-1609, doi: 10.1175/JAMC-D-12-0204.1,2013.~~

Seinfeld, J. H., and S. N. Pandis (1998), Atmospheric chemistry and physics, Wiley-Interscience.

Seibert, P., Beyrich, F., Gryningc, S.-E.,Joffred, S., Rasmussene, A., Tercierf,P.: Review and intercomparison of operational methods for the determination of the mixing height. Atmospheric Environment, 34(7), 1001–1027, doi: 10.1016/S1352-2310(99)00349-0, 2000.

Mis en forme : Anglais (Royaume-Uni)

Mis en forme : Police :(Par défaut) Times New Roman, 10 pt, Anglais (Royaume-Uni)

Mis en forme : Police :(Par défaut) Times New Roman, 10 pt, Anglais (Royaume-Uni)

Mis en forme : Police :(Par défaut) Times New Roman, 10 pt, Anglais (Royaume-Uni)

Mis en forme : Police :(Par défaut) Times New Roman, 10 pt, Anglais (Royaume-Uni)

Mis en forme : Police :(Par défaut) Times New Roman, 10 pt, Anglais (Royaume-Uni)

Mis en forme : Police :(Par défaut) Times New Roman, 10 pt, Anglais (Royaume-Uni)

Mis en forme : Anglais (Royaume-Uni)

Mis en forme : Anglais (Royaume-Uni)

Mis en forme : Anglais (Royaume-Uni)

Mis en forme : Anglais (Royaume-Uni)

Mis en forme : Anglais (Royaume-Uni)

Mis en forme : Anglais (Royaume-Uni)

Sicard, M., Barragan, R., Dulac, F., Alados-Arboledas, L., and Mallet, M.: Aerosol optical, microphysical and radiative properties at three regional background insular sites in the western Mediterranean Basin, Atmos. Chem. Phys. Discuss., doi:10.5194/acp-2015-823, in review, 2016.

Skamarock, W. C., Klemp, J. B., Dudhia, J., Gill, D. O., Barker, D. M., Duda, M., Huang, X.-Y., Wang, W. and Powers, J. G.:, A description of the advanced research WRF version 3, NCAR Technical Note, 2008.

Stull, R. B.: An Introduction to Boundary Layer Meteorology, Kluwer Academic Publishers, 1988.

Stull, R. B.: Meteorology: For Scientists and Engineers, Thomson Learning, 2000.

Summa, D., Di Girolamo, P., Stelitano, D., and Cacciani, M.: Characterization of the planetary boundary layer height and structure by Raman lidar: comparison of different approaches. Atmospheric Measurement Techniques, 6(12), 3515–3525,doi: 10.5194/amt-6-3515-2013, 2013.

Titos, G., Foyo-Moreno, I., Lyamani, H., Querol, X., Alastuey, A., and Alados-Arboledas, L.: Optical properties and chemical composition of aerosol particles at an urban location: An estimation of the aerosol mass scattering and absorption efficiencies. Journal of Geophysical Research Atmospheres, 117(4), 1–12,doi: 10.1029/2011JD016671, 2012.

Valenzuela, A., Olmo, F. J., Lyamani, H., Antón, M., Quirantes, A., and Alados-Arboledas, L.: Aerosol radiative forcing during African desert dust events (2005–2010) over Southeastern Spain, Atmos. Chem. Phys., 12, 10331-10351, doi:10.5194/acp-12-10331-2012, 2012.

Wang, Z., Cao, X., Zhang, L., Notholt, J., Zhou, B., Liu, R., and Zhang, B.: Lidar measurement of planetary boundary layer height and comparison with microwave profiling radiometer observation. Atmospheric Measurement Techniques, 5(8), 1965–1972, doi: 10.5194/amt-5-1965-2012, 2012.

Xie, B., Fung, J. C. H., Chan, A., and Lau, A.: Evaluation of nonlocal and local planetary boundary layer schemes in the WRF model. Journal of Geophysical Research Atmospheres, 117(12), 1–26, doi: 10.1029/2011JD017080, 2012.

Mis en forme : Anglais (Royaume-Uni)

Mis en forme : Anglais (Royaume-Uni)

Mis en forme : Anglais (Royaume-Uni)

Table 1: R^2 among z_{PBL}^{POL}, z_{PBL}^{MWR} and z_{PBL}^{WRF} during ChArMEx 2012 and 2013. Points are the number of values used to retrieve the correlation factor. $\overline{\Delta_{PBL}^{POL-WRF}}$, $\overline{\Delta_{PBL}^{MWR-WRF}}$, and $\overline{\Delta_{PBL}^{POL-MWR}}$ are the mean differences between the z_{PBL}^{POL}, z_{PBL}^{MWR}, and z_{PBL}^{MWR}. Daytime is considered between 06:00 and 19:00 UTC (PBL means the ML) and night-time is the rest of the day (PBL means the RS).

		Daytime	$R^2_{POL-WRF}$	Points	$\overline{\Delta_{PBL}^{POL-WRF}}$(m)	$R^2_{MWR-WRF}$	Points	$\overline{\Delta_{PBL}^{MWR-WRF}}$(m)	$R^2_{POL-MWR}$	Points	$\overline{\Delta_{PBL}^{POL-MWR}}$(m)
ChArMEx	2012	9th July	0.236	12	850	0.664	12	440	0.598	12	380
		10th July	0.763	26	680	0.605	26	410	0.718	26	240
		11th July	0.661	26	1170	0.441	26	520	0.361	26	1700
	2013	16th June	0.122	26	830	0.395	26	1330	0.803	26	570
		17th July	0.018	26	422	0.094	26	280	0.304	26	40
		Night-time	$R^2_{POL-WRF}$	Points	$\overline{\Delta_{PBL}^{POL-WRF}}$(m)	$R^2_{MWR-WRF}$	Points	$\overline{\Delta_{PBL}^{MWR-WRF}}$(m)	$R^2_{POL-MWR}$	Points	$\overline{\Delta_{PBL}^{POL-MWR}}$(m)
	2012	9th July	0.660	28	940	0.364	17	190	0.463	17	1150
		10th July	0.640	28	930	0.032	9	180	0.057	9	1130
		11th July	0.440	28	770	0.230	11	380	0.062	11	1130
	2013	16th June	0.030	28	390	0.099	9	400	0.028	9	730

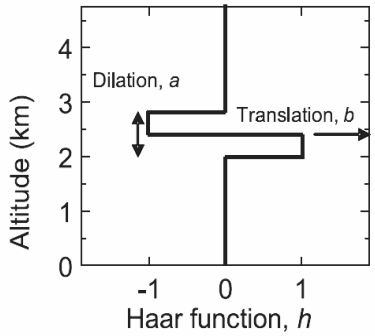

Figure 1: Haar's function defined by the dilation (a) and the translation (b).

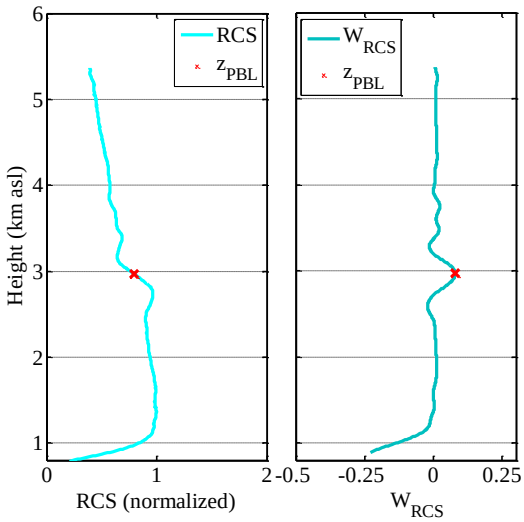

Figure 2: Example of a normalized RCS and its wavelet covariance transform. Red cross indicates the possible location of the PBL height.

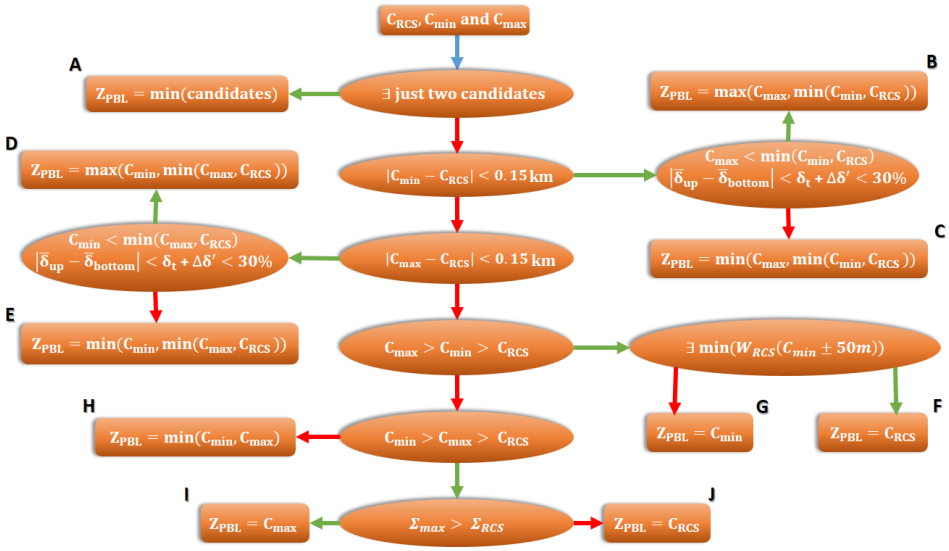

Figure 3: Flux diagram of the algorithm used by POLARIS to determine the z_{PBL}. C_{min}, C_{max} and C_{RCS} are the candidates. The blue arrow indicates the start. Conditions are marked in ellipses and the final attribution of the z_{PBL} in rectangles. The green and red arrows indicate the compliance and noncompliance of the conditions, respectively. The rest of the symbols are explained in the text.

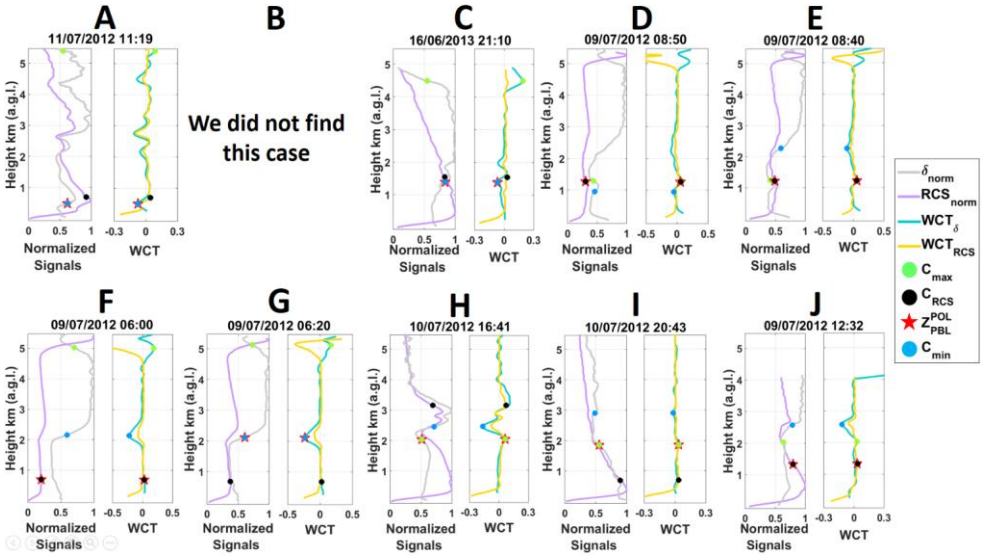

Figure 4: Examples of the cases mentioned in Figure 3 occurred during ChArMEx 2012 and 2013. Normalized RCS (violet line) and δ (grey line) are shown in left axis and WCT of RCS (yellow line) and δ (ligh blue line) are shown in right axis. C_{min} (blue dot), C_{max} (green dot), C_{RCS} (black dot) and the final attribution z_{PBL}^{POL} (red start) are shown in both axis.

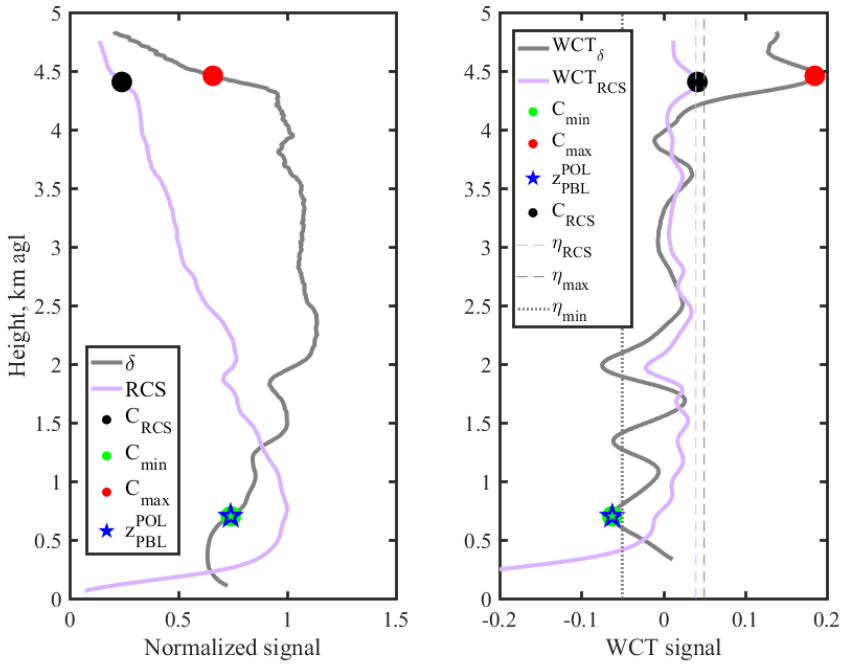

Figure 5: Normalized RCS and δ profiles (left). WCT of the RCS, δ and thresholds η_{min} (–0.05) and η_{RCS} (0.05), η_{max} (0.04) (right) at 21:30 UTC 16 June 2013. C_{CRS}, C_{min} and C_{max} candidates and z_{PBL}^{POL} are shown in both axes.

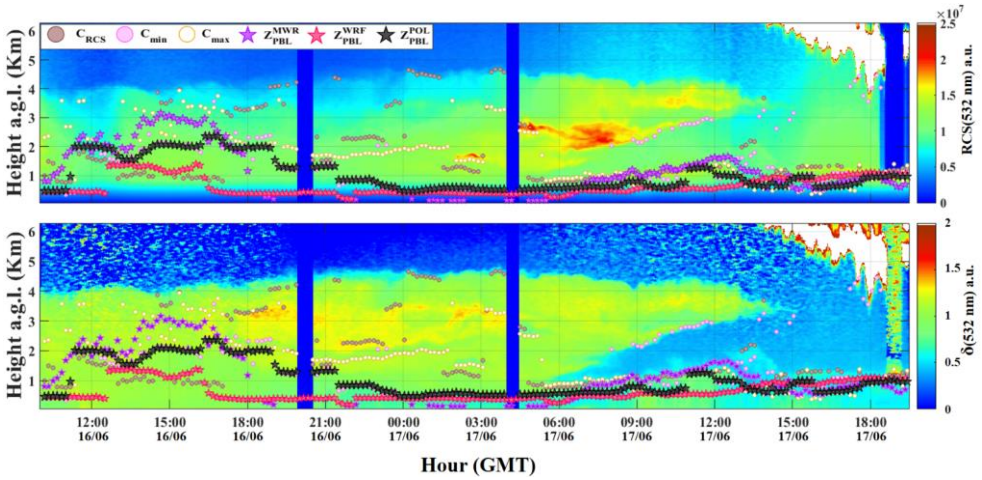

Figure 6: Temporal evolution of the range corrected signal (RCS) (top) and the perpendicular-to-parallel signal ratio (δ) (bottom) in the period 09:00 16 June - 20:00 17 June 2013 (colour maps). The scatter plots represent the candidate for z_{PBL}: C_{RCS} (brown dot), C_{min} (pink dot) and C_{max} (ochre dot). The z_{PBL} determined with POLARIS (black star), by the parcel method using MWR measurements (violet star) and derived from WRF model (red star). Measure gaps are dark-current measurements.

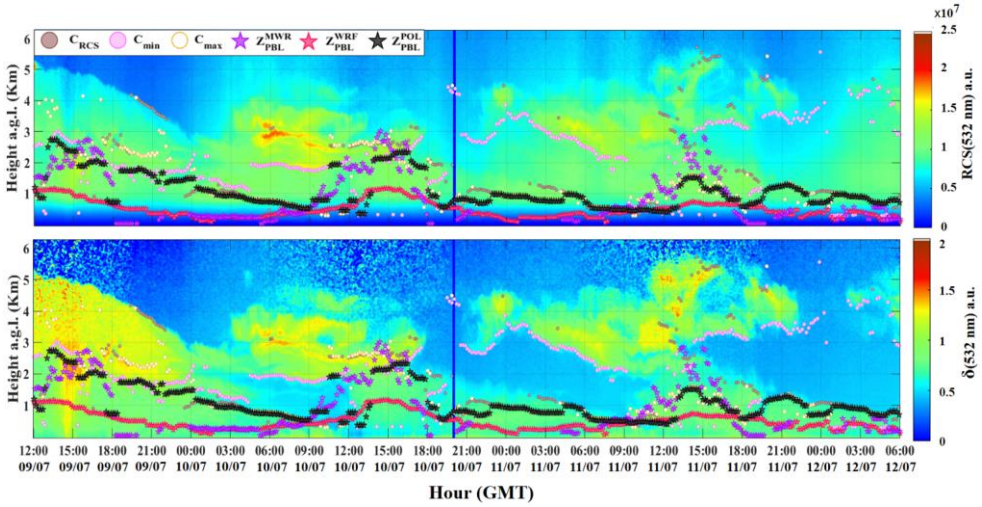

Figure 7: Temporal evolution of the range corrected signal (RCS) (top) and the perpendicular-to-parallel signal ratio (δ) (bottom) in the period 12:00 9 July – 06:00 12 July 2012 (colour maps). The scatter plots represent the candidate for z_{PBL}: C_{RCS} (brown dot), C_{min} (pink dot) and C_{max} (ochre dot). The z_{PBL} determined with POLARIS (black star), by the parcel method using MWR measurements (violet star) and derived from WRF model (red star). Measure gap is dark-current measurement.